Chemical aging of atmospheric mineral dust during transatlantic transport

Mohamed Abdelkader[1], Swen Metzger[1,2], Benedikt Steil[1], Klaus Klingmüller[1], Holger Tost[3],
Andrea Pozzer[1], Georgiy Stenchikov[4], Leonard Barrie[5], and Jos Lelieveld[1,2]

[1]Air Chemistry Department, Max Planck Institute for Chemistry, Mainz, 55128, Germany
[2]Energy, Environment and Water Research Center, The Cyprus Institute, Nicosia, 2121, Cyprus
[3]Institute for Physics of the Atmosphere, Johannes Gutenberg University, Mainz, 55099, Germany
[4]King Abdullah University of Science and Technology, Thuwal 23955-6900, Saudi Arabia
[5]Department of Geological Sciences, Stockholm University, Stockholm, SE-106 91, Sweden

Correspondence to: M. Abdelkader (m.abdelkader@mpic.de), S. Metzger (s.metzger@cyi.ac.cy)

Abstract. Transatlantic dust transport has many implications for the atmosphere, ocean and climate. We present a modeling study on the impact of the key processes (dust emissions flux, convection and dust aging parameterizations) that control the transatlantic dust transport. Typically, the Inter-Tropical Convergence Zone (ITCZ) acts as a barrier for the meridional dust transport. To characterize the dust outflow over the Atlantic Ocean, we address two regional phenomena: (i) dust interactions with the ITCZ (DIZ) and (ii) the adjacent dust transport over the Atlantic Ocean (DTA). In the DTA zone, the dust loading shows a steep and linear gradient westward over the Atlantic Ocean where particle sedimentation is the dominant removal process, whereas in the DIZ zone cloud interactions and wet deposition predominate. To study the different impacts of aging, we present two case studies that exclude condensation and coagulation, and include dust aging at various levels of complexity. For dust aging, we consider the uptake of inorganic acids on the surface of mineral particles that form salt compounds. Calcium, used as a proxy for the overall chemically reactive dust fraction, drives the dust-related neutralization reactions leading to higher dust aerosol optical depth (AOD). The aged dust particles are transferred to the soluble aerosol modes in the model and are mixed with other species that originate from anthropogenic and natural sources. The neutralization products (salts) take up water vapor from the atmosphere and increase the dust AOD under subsaturated conditions. We define the *"direct effect of dust aging"* to refer to the increase in AOD as a result of hygroscopic growth. On the other hand, the aged dust is more efficiently removed (wet and dry) because of the increase in particle size and hygroscopicity. This more efficient removal reduces the dust AOD over the DIZ zone. We define this as the *"indirect effect of dust aging"*, complementary to the direct effect that is dominant in the DTA zone. Distinction of the two aging effects helps develop insight into the regional importance of dust–air-pollution interactions.

1 Introduction

In the past several decades, transatlantic dust transport has gained tremendous attention because of many important impacts on Earth's climate, human health and ecosystems. North African dust transport over the Atlantic Ocean has emerged as a major

Atmospheric
Chemistry
and Physics
Discussions

contributor to the soil nutrient input to many islands in the Caribbean, the Bahamas (Muhs et al., 2007), Bermuda (Muhs et al., 2012) and in Amazon Basin (Bristow et al., 2010; Ben-Ami et al., 2012; Abouchami et al., 2013). Dust deposition influences the oceanic and terrestrial biogeochemistry by the transport of nutrients such as iron (Ussher et al., 2013; Baker et al., 2013, 2010; Jickells et al., 2005) and phosphorus (Nenes et al., 2011) that efficiently dissolve into the ocean. The emission, transport, and

5   deposition processes of the North African dust are strongly influenced by meteorology causing strong seasonal, inter-annual and decadal variability (Mahowald, 2007; Mahowald et al., 2010). Large fractions of the dust emissions are carried across the west coast of North Africa up to the Western Atlantic (Prospero et al., 2014) and significant correlations exist between the dust and climate variables, such as sea surface temperature, the North Atlantic Oscillation (NAO), and the Madden-Julian Oscillation (MJO) (Ginoux et al., 2004; Wong et al., 2008; Guo et al., 2013). In addition, the African dust in the Sahara air-

10 layer region influences the rates of rainfall in the Inter-Topical Convergence Zone (ITCZ) (Huang et al., 2009, 2010), and its radiative impacts shifted and widened the ITCZ northward (Bangalath and Stenchikov, 2015).

African dust is transported in great quantities to the Caribbean basin throughout the year, although the strong seasonal cycle shows the maximum transport of the dust in boreal summer and the minimum in winter (Prospero et al., 2014; Yu et al., 2015). The seasonality is corroborated by satellite measurements of aerosol optical depth (AOD), which show huge plumes of high

15 AOD in summer extending from the west coast of Africa to the Caribbean, the Gulf of Mexico, and to the southern United States (Hsu et al., 2012; Yu et al., 2013; Chin et al., 2014; Kim et al., 2014; Groß et al., 2015). The satellite data indicate that the dust transport to the Western Atlantic in winter and spring is comparable, but the dust is largely confined to the southern latitudes of Barbados with a plume axis crossing the coast of South America in the region of French Guiana and Surinam. In addition, satellite data indicate a decrease of 50% in AOD and a decrease of 0.1–0.2 in the dust-only optical depth during the

20 transport (Kim et al., 2014). The ITCZ acts as an efficient removal mechanism (Prospero et al., 2014) and thus as a barrier to the transport of dust to the southern Atlantic (Huang et al., 2009, 2010; Adams et al., 2012). To characterize the transatlantic dust transport, many studies have used satellite observations (Liu et al., 2008; Ben-Ami et al., 2009, 2010; Adams et al., 2012; Ben-Ami et al., 2012; Ridley et al., 2013; Alizadeh-Choobari et al., 2014; Kim et al., 2014; Yu et al., 2015, among others). However, the estimation of the satellite-based dust flux has large uncertainties, primarily because of uncertainties associated

25 with the derived dust-only optical depth (Yu et al., 2009, 2013) and the dust mass extinction efficiency. Both parameters are used for calculating the dust mass loading (Kaufman, 2005).

Therefore, the modeling of the dust cycle and the associated impacts are found to be challenging for global and regional models because the complex dust processes have to be parameterized using a suite of simplifications (Astitha et al., 2010; Nowottnick et al., 2010; Huneeus et al., 2011; Ridley et al., 2013; Kim et al., 2014; Gläser et al., 2015, among others).

30 Although most sophisticated atmospheric models can reproduce the transatlantic dust transport plumes , but the patterns differ in magnitude and seasonality. Generally, the models show better performance in summer than in winter for the transatlantic dust transport (Huneeus et al., 2011). It has been observed that large uncertainties particularly exist between model simulations of the dust deposition (wet and dry) (Schulz et al., 2012). The atmospheric models that are applied in the AeroCom model intercomparison activity (http://aerocom.met.no/) show that the mean normalized bias of the AOD model varies within a wide

35 range from –0.44 to 0.27 (Huneeus et al., 2011)), which is caused by large discrepancies in the dust-related processes (emission

Atmospheric
Chemistry
and Physics
Discussions

and horizontal and vertical distributions) that affect the dust transport from Northern Africa over the Atlantic ocean (Prospero et al., 2010). This indicates that in present models the dust removal is very efficient during the transatlantic dust transport (Kim et al., 2014) and that the development of the model requires a more comprehensive representation of the dust processes. Though the incorporation of the satellite products helps in improving the modeling results, a deeper understanding of the key

5   factors that determine the transport of the dust is also required. This study aims at examining the factors that can affect the transatlantic dust transport by explicitly considering the chemical aging of the mineral dust during long-range transport in a state-of-the-art atmospheric chemistry climate model setup.

2   Model Description

We have used the EMAC (The ECHAM5/MESSy2 atmospheric chemistry General Circulation Model) in a setup following

10   Abdelkader et al. (2015). The EMAC model describes the tropospheric and middle atmosphere processes and their interactions with land and oceans considering various submodels (Joeckel et al., 2010). The mineral dust particles are emitted in two log-normal distribution modes (accumulation and coarse) with median diameters of 0.5 μm and 5.0 μm and a modal standard deviation of 1.59 and 2.0 for the accumulation and coarse modes respectively (Abdelkader et al., 2015). The anthropogenic emissions are based on EDGARv4.0 inventory (Pozzer et al., 2012) and include the greenhouse gases, NO_x, CO, non-methane

15   volatile organic compounds (NMVOCs), NH_3, SO_2, black carbon (BC) and organic carbon (OC) from fossil fuel and biofuel use. The monthly large-scale biomass burning emissions of OC, BC and SO_2, are based on GFED version 3 (Global Fire Emissions Database) (van der Werf et al., 2010). The emissions drive a comprehensive atmospheric chemistry mechanism (Sander et al., 2005), which calculates major inorganic acids (H_2SO_4, HNO_3, HCl) online with meteorology. Organic acids are not considered in this model setup since their concentrations over Sahara during dust outflow are very low, however, many

20   modeling studies reported the uptake of organic acids by dust particles (Metzger et al., 2006; Möhler et al., 2008; Liu et al., 2013; Alexander et al., 2015; Wang et al., 2015; Alexander et al., 2015).

    The chemical aging of the dust depends on the condensation of inorganic acids and the associated uptake of water vapor. Considering inorganic acids increases the level of dust aging, water uptake, particle size, removal rate and eventually may further decrease the dust lifetime. The condensation of acids yields anions, i.e., sulfate (SO_4^{2-}), bi-sulfate (HSO_4^-), nitrate

25   (NO_3^-), and chloride (Cl^-), whereas the condensation of ammonia (NH_3) yields a semi-volatile cation, ammonium (NH_4^+) that reacts with the inorganic anions in competition with the mineral cations Na^+, Ca^{2+}, K^+, Mg^{2+} (Metzger et al., 2006). However, in this study the cations are considered as reactivity proxy for natural aerosols, such as sea salt, biomass burning, or mineral dust. The anion–cation neutralization products (salt compounds), simulated by the ISORROPIA-II aerosol thermo-dynamics model (Fountoukis and Nenes, 2007), can alter the hygroscopicity of the atmospheric dust particles, but the effect

30   strongly depends on the atmospheric residence time, region, and concentration of acids. Generally, dust aging changes the solubility, which controls the water uptake and in turn alters the aerosol size distribution (Metzger et al., 2006). The latter is a key parameter and important for aerosol-radiation feedback, aerosol in-cloud processing (nucleation scavenging), and below-cloud (impaction) scavenging. Our scavenging processes include detailed pH-dependent aqueous phase chemistry (Tost et al., 2006a)

which is fully coupled with the aerosol and gas-phase chemistry, liquid cloud water, and ice crystals. In addition to the aerosol hygroscopic growth and scavenging, the dust size distribution can change by coagulation, and smaller particles can grow into larger sizes for both the soluble and insoluble aerosol modes (Pringle et al., 2010). Aerosol hygroscopic growth is only allowed in the soluble modes (Abdelkader et al., 2015). Dry deposition and particle sedimentation can remove all particles from the atmosphere (Kerkweg et al., 2006). Thus, the representation of the dust cycle in our EMAC setup couples the dust emissions, loading, and lifetime with the radiative forcing. As a result, changes in the dust loading feed back to the surface wind speed, soil moisture, cloud formation and precipitation, and in turn the dust emission flux. Overall, the level of air pollution controls the dust cycle because it determines the level of dust aging by inorganic acids and water vapor. A Newtonian relaxation approach is used to nudge the model meteorology in the free atmosphere (i.e., above the boundary layer) to achieve a realistic simulation of the surface wind speed and tracer transport (Abdelkader et al., 2015). Nudging significantly improves the surface dust mass concentration over the Caribbean compared with dust observations (Astitha et al., 2012). The model spectral resolution is T106 (≈ 110 km) and for the longterm simulations it is T42 (≈ 280 km). Both model resolutions use 31 vertical levels. Figure 1 summarizes the representation of the dust cycle and air-pollution-dust-aging-radiation feedbacks in our EMAC setup.

3 Long-term evaluation

This study aims at examining the key factors that affect the transatlantic dust transport considering a comprehensive model evaluation for the period 2000–2012 with a model resolution of T42 (≈ 280 km). For the model evaluation, we use the following satellite and ground station AOD products:

- AErosol RObotic NETwork (AERONET) (Holben et al., 1998);

- Cloud-Aerosol Lidar and Infrared Pathfinder Satellite Observations (CALIPSO) (Winker et al., 2009, 2007);

- MODerate resolution Imaging Spectroradiometer (MODIS) platforms Aqua and Terra (product collection 6, L3 gridded data, Kaufman et al. (1997));

- Precipitation data from Tropical Rainfall Measuring Mission (TRMM) (product version 31 L3 gridded data, Diner et al. (1998));

Figure 2 shows the seasonal average of the modeled dust burden and the precipitation rate over a 13-year simulation period. Both the dust burden and the precipitation rate peak during the summer season (JJA), where the dust plume is located relatively far north from the equator, in agreement with remote sensing observations (Prospero et al., 2014; Yu et al., 2015). During the winter season (DJF), the dust burden and the precipitation rate show a minimum, whereas during the spring season (MAM), the dust plume and the ITCZ are shifted southward. In winter and spring, the dust transport shifts southward to 0°-10°N and affects South America significantly, whereas during summer, the dust transport occurs predominantly at 10°-20°N, substantially affecting the Caribbean (Yu et al., 2015). During boreal winter the enhanced precipitation over the Northern part of South America results in higher and localized dust scavenging because the precipitation along the dust transport from the

Western Africa into the Caribbean is at minimum. In contrast, during boreal summer, the dust spreads to a larger extent into the ITCZ because of the stronger dust emissions (Prospero et al., 2014) and is associated with enhanced dust scavenging. The strong southward gradient of the dust burden ($\approx 100 \, \mathrm{mg \, m^{-2} \, deg^{-1}}$) is collocated with precipitation in the western part of the Sahel and the ITCZ region. During the winter months, dust is primarily scavenged over Southeast America. As a result, the

5   extent of the dust outflow is primarily affected by the precipitation in the ITCZ region. Figure S1 in the Supplement shows the dry and the wet removal of the dust particles. It shows that the dry removal dominates the northern part of the dust outflow region, whereas the wet removal dominates the southern part. To indicate the region where the dust interacts with the ITCZ, we introduce the dust-ITCZ (DIZ) zone. In this region, for the transatlantic dust transport, the dust and cloud interactions are more important and the dust scavenging is very efficient. We refer to the region where the sedimentation and the dry deposition

10   dominate the dust removal as the adjacent dust transport over the Atlantic Ocean (DTA) zone.

     Figure 3 shows the DIZ and DTA zones, and the AERONET stations used in this study to evaluate the modeled AOD. The area bounded by the blue line represents the area where the dust interacts with the ITCZ. This region largely controls the transport of the dust into Caribbean (Doherty et al., 2012, 2014), and therefore in this study it is introduced as the DIZ zone to illustrate the modeled transatlantic dust transport.

15   Figure 4 summarizes the long-term evaluation results for the transatlantic dust transport. The figure compares the modeled AOD with the AERONET observations and shows (i) the transatlantic dust transport region with skill scores at each station (see Appendix A), (ii) the time series of the six selected stations that provide long-term data with three stations each in the Caribbean (left) and around the Western Africa (right) (for the station locations see Figure 3), and (iii) the corresponding scatter plots for both sides of the Atlantic Ocean. Table 1 summarizes the model performance for both regions over the entire period (2000–

20   2012). The 13-year average (based on 5 hours intervals) of the modeled AOD for the Western Africa sites is 0.16±0.27 (one standard deviation), which is comparable to the observation of 0.24±0.37. However, the difference is larger compared with the Caribbean sites, which is represented by an average modeled AOD of 0.12±0.18 and with 0.14±0.22 by the observations. At both sides of the Atlantic, the lower variability of the model is primarily a result of the relatively coarse model resolution (280 km), which was used for these long-term simulations because of higher computation cost of the higher resolution. The skill

25   score (SS1 (Taylor, 2001)) has a value of 0.73 and 0.70 for the Western Africa and the Caribbean sites, respectively. A rather good comparison is shown by the correlation coefficients (R) although the values are lower because R is more phase sensitive than the SS1, i.e., more sensitive to time lags between modeled and observed AOD. The higher R value for Western Africa (0.61) compared with the Caribbean (0.41) results from the overall higher dust AOD contribution to the total AOD, compared with the Caribbean. Typically, the Caribbean is strongly influenced by the uncertainty of the long-range transport and the

30   associated dust aging (with potential failures causing a time shift of the dust peaks during the transport). These differences are best described by time series. Overall, the model captures the variability of AOD at all stations, but around Western Africa the model underestimates the AOD peaks, especially at Dakar which is on the edge of the DIZ zone. Over the Caribbean, the model seems to agree slightly better but it generally underestimates the AOD during the dust outflow periods, e.g., seen at the AERONET station La Parguera. This underestimation could be either caused by an insufficient representation of the dust

35   emissions and the related processes in the source region of the Western Africa (Huneeus et al., 2011; Shao et al., 2011; Cuevas

et al., 2015), an overestimated removal during the transport (Schulz et al., 2012; Prospero et al., 2014), or insufficient dust transport from the boundary layer into the free atmosphere (Khan et al., 2015). In addition, the underestimation of the AOD could be due to the missing large coarse particles (larger than $10\,\mu m$) in the model, which could lead to the underestimation of AOD on the Western Africa side whereas these large particles are not transported over long distances. In this study, we focus on the sensitivity of the emission flux and the removal mechanisms, whereas the effect of large coarse particles and their radiative forcing is a subject of future study.

4 Sensitivity studies

To resolve the impact of various key factors that control the dust modeling, we focus on a period with relatively strong dust outflow that occurred during July 2009 with a surface concentration up to $600\,\mu g\,m^{-3}$ at Dakar, as indicated by monthly mean AOD observations at Dakar and Capo Verde (highlighted by the red bar in Fig. 4). For this month, the model and observations show a relatively large difference and therefore this period is suitable to test various model parameters that may affect the transatlantic dust transport, i.e., (a) the dust emission flux, (b) the convective parameterization, and (c) the level of dust chemical aging. The sensitivity studies conducted using EMAC are all based on a higher spectral resolution than the long-term evaluation (i.e., T106, or $\approx 110\,km$). Table 1a and table 1b in the supplement show the evaluation metrics for the AOD for sensitivity studies over West Africa and the Caribbean, respectively.

During the transatlantic dust transport, the ITCZ represents a strong barrier for the dust outflow and therefore controls the meridional extent of the dust plume (Yu et al., 2015). The ITCZ acts as a major sink that depends on the amount of precipitation (Prospero et al., 2014; Schlosser et al., 2014) and the removal might be enhanced depending on the dust aging (Abdelkader et al., 2015). Figure 5 shows the dust burden and the total mean precipitation for July 2009 using the reference EMAC simulation, which includes the dust cycle and aging as shown in Fig. 1. Generally, two strong precipitation areas are visible with one peak centered at 15°W with a monthly average of $20\,mm\,day^{-1}$, i.e., one at the coast of West Africa and the other peak area is located in the Caribbean at 50°W. with a monthly average of $25\,mm\,day^{-1}$ These precipitation maxima influence the dust loading. The precipitation within the ITCZ coincides with the steep gradient of the dust burden in the meridional direction over the Western Africa. Along the zonal extent of the dust plume, the collocation of the dust plume and precipitation indicates that the meridional extent of the dust is primarily affected by the location of the ITCZ. Fig. S1 in the Supplement summarizes the monthly average dust removal during July 2009.

Figure 6 shows the time series of the size-resolved surface dust concentrations. Two main dust outflows on the 2nd and 12th July are simulated at the Capo Verde station, indicated by dust concentrations higher than or close to $300\,\mu g\,m^{-3}$ (equivalent particle cutoff diameter of $5\,\mu m$) and another weaker dust outflow is simulated on 24th July, indicated by a lower concentration peak around $100\,\mu g\,m^{-3}$. The former two dust outflows are seen at Dakar with twice the concentration (up to $600\,\mu g\,m^{-3}$) at slightly different times due to different transport. These dust outflows reach the Caribbean ≈ 5 days later, with a significant lower surface concentration of around $60\,\mu g\,m^{-3}$. Despite chemical aging, the model concentrations show a majority of the dust particles in the insoluble coarse (ci) mode, which indicates that the dust particle concentration is high or the level of

Atmospheric
Chemistry
and Physics
Discussions

inorganic acids is low, not allowing for complete aging. This is especially valid for high dust outflows. On the other hand, the fraction of the aged dust (cs/ci) is somewhat higher in the Caribbean because of the continuous aging during long-range transport. The aged dust fraction over West Africa is about 10% of the total dust mass and twice of that at the Caribbean sites. The same is true for the dust in the accumulation modes (ai and as), but the mass concentrations are an order of magnitude

5 lower compared with the coarse mode concentration and therefore they are not visible at the linear scale. At higher elevations, this fraction can be different because of different dust and precursor gas concentrations.

To investigate the vertical distribution, the modeled dust extinction is compared with the dust subtype classification of the CALIPSO retrievals. Figure 7 shows a comparison for the second dust outbreak on 12 July 2009. The figure shows a subset of four collected CALIPSO tracks and includes a qualitative comparison of the dust layer height. The scatter plot attached to each

10 panel represents the point-to-point comparison, colored by the height of each observation point whereas the area plots show the dust burden interpolated in time to the CALIPSO overpass time which is indicated by a solid black line. Additional CALIPSO tracks are shown in Fig. S2a–Fig. S2e in the Supplement. Both EMAC and CALIPSO show that the dust over the Sahara reaches an elevation up to 7 km. The dust burden is very low (as indicated by the area plot) south of 10°N, which coincides with a very low AOD observed by CALIPSO. Both EMAC and CALIPSO shows that the dust plume is limited to the area

15 between 14° to 22°N and the top of the dust layer is reduced to 5 km in the middle of the Atlantic. This is primarily a result of the prevailing deposition (gravitational settling + wet removal), which is further discussed in the following sections. Once the dust reaches the Caribbean, the plume spreads over a considerably larger area, which extends 5° to 28°N as a result of change in meteorological conditions. The dust plume eventually reaches the Caribbean with a top layer height of ≈ 5 km. In Fig. 7, the comparison with CALIPSO (and Fig. S2a–Fig. S2e in the supplement) shows that the model nicely captures the vertical

20 structure of the dust outbreak during the transport over the Atlantic Ocean. Nevertheless, the model tends to systematically overestimate the dust extinction at lower altitudes, whereas at higher altitudes the model tends to underestimate the CALIPSO extinction (considering all CALIPSO tracks in Fig. 7 and Fig. S2a–Fig. S2e in the Supplement). This indicates that EMAC might remove the dust too efficiently during transport. The reason can be manifold and caused by different insufficiently represented processes of the dust cycle (Figure 1). Next, the key factors are investigated.

25 ## 4.1 Dust emission flux

A successful representation of the dust cycle depends on an accurate dust emission flux. However, the correctness of the modeled emission flux critically depends on many model parameters, where some of them are resolution dependent. Using EMAC, the dust emissions are calculated considering the frictional velocity following Astitha et al. (2012). To test the sensitivity of the transatlantic dust transport to the dust emission parameterization, several sensitivity simulations were performed, which are

30 summarized in Table 2. The dust mass emitted during July 2009 within the region between 20°W to 10°E and 15°N to 30°N for the reference case is 0.6133 kg m^{-2}.

The first test case (B1E1) represents a redistribution of emission bins between the coarse and accumulation modes so that dust particles are shifted from the coarse to the accumulation mode while conserving the total dust mass. In this case, a higher amount of dust in the accumulation mode is transported over larger distances compared with the reference case "EMAC".

Atmospheric
Chemistry
and Physics
Discussions

"EMAC" considers the same total dust mass with a larger fraction in the coarse mode. Additional sensitivity runs, B1E2 to B1E7, change the total dust emission flux by increasing the emission flux according to different factors shown in Table 2. The horizontal dust emission flux is described by Eq. 1 (Marticorena and Bergametti, 1995; Astitha et al., 2012)

$$H = \frac{c\rho_{air}u_*^3}{g}(1+\frac{u_t^*}{u^*})(1-\frac{u_t^{*2}}{u^{*2}}), u^* > u_t^* \tag{1}$$

5   With the tuning parameter c = 1 representing the reference case "EMAC" following (Darmenova et al., 2009; Astitha et al., 2012), g is the gravitational acceleration, ρ_{air} the air density, u^* the friction velocity, u_t^* the threshold friction velocity. For case B1E8, the horizontal mass flux is increased by a factor of 2.6 – as this is another "tuning" factor for the emission scheme (parameter c in Eq. 1). The cases highlighted in Table 2 are shown in Fig. 8, whereas the other cases are shown in the Supplement (Fig. S3).

10   Due to the different dry and wet deposition characteristics of the accumulation and coarse mode particles, significant differences might be expected. Figure 8 shows that the AOD time series at the selected AERONET stations are rather insensitive to the emission flux modifications except for case B1E3 (and B1E4, which is shown in the Supplement). This is valid for both sides of the Atlantic, where the AOD at the Caribbean stations seems even less sensitive than the AOD for the Western Africa sites. Only for the cases where the coarse mass flux is significantly increased (factor of 5.3), the AOD shows a higher

15   sensitivity. The large increase in the coarse mode mass for case B1E3 results in a significant increase in AOD (exceeding 2.0) on both sides of the Atlantic Ocean. Case B1E8 (modification of the horizontal mass flux) shows better agreement with the AERONET observations at both sides of the Atlantic Ocean despite the very high AOD values obtained on 21 July at Saada station. The model captures the AOD during the two dust outflow events (2 July and 12 July) at Capo Verde as well as the first dust outflow at Saada on 4 July. For the Caribbean sites, case B1E8 shows the best agreement with AERONET for the three

20   stations.

The sensitivity simulations show that the accumulation mode fraction of the dust contributes much less to the AOD on both sides of the Atlantic Ocean because even an increase by a factor of 5.3 in the dust emission flux is not sufficient to match the observations. Instead, such an increase (by a factor of 5.3) in the emitted dust mass flux results–regionally and globally–in an unreasonable dust budget shown by Astitha et al. (2012). On the other hand, this sensitivity study shows that

25   the AOD is more sensitive to the dust mass in the coarse mode and that the AOD over the Caribbean is much less sensitive to the total dust emission flux. Clearly, the model sensitivity is higher for the West African sites because these AOD results are primarily controlled by the Saharan dust outbreaks. To match the elevation at which this outflow occurs is also important as the comparison with the CALIPSO observations showed (Fig. 7) providing that EMAC overestimates the dust extinction at lower elevations whereas it underestimates the values at higher elevations. Instead, for long-range transport, this finding points to the

30   strong contribution of the dust removal on the transatlantic dust transport.

4.2   Convection schemes

The scavenging of dust particles by precipitation is another key factor that controls the transatlantic dust transport (Kim et al., 2014). In order to study the impact of the convection and the associated precipitation during the dust outflow, different convec-

Atmospheric
Chemistry
and Physics
Discussions

tion schemes that are implemented by Tost et al. (2006b) in the EMAC model are compared. Different convection parameteri-
zation schemes have been evaluated and the default scheme (TIEDTKE convection with NORDENG closure) provides realistic

5   water vapor distributions on the global scale, which is crucial for radiative transfer processes and atmospheric chemistry (Tost
et al., 2006b, 2010; Rybka and Tost, 2013). Table 2 presents the sensitivity tests by using the available convective schemes of
the EMAC model. The principal cases are shown in Fig. 9, whereas the other cases are shown in the Supplement (Fig. S4).

Figure 9 demonstrates that the AOD time series for the stations shown in Fig. 3 are more sensitive to the convection pa-
rameterization than to the emission flux parameterizations (Sec. 4.1). For the convection parameterization, the AOD is more

10 sensitive over West Africa than over the Caribbean sites, which is primarily a result of the decreasing dust burden due to the
removal of the dust during transport (Fig. 6). Generally, the AOD is underestimated at all stations, except for Saada, for the
reference simulation (EMAC), which is significantly improved for the sensitivity simulations (B1T3 and B1T5) during the pe-
riod 20–25 July 2009. During this period, the model simulates a dust outflow, which is not shown by AERONET observations.
Over the Caribbean, case B1T5 (ECMWF operational convection scheme) shows better results for all dust outflow events.

15 Generally, the main differences between the schemes appear in the tropical region, and the maximum difference is obtained
during the boreal summer. For these conditions (location + time), the EMAC reference setup shows the maximum difference in
the precipitation amount (Tost et al., 2006b). As a result, the scavenging of aerosols, including dust particles, is overestimated
due to the high precipitation rates. Consequently, this over-removal of the dust results in an underestimation of the AOD over
the Caribbean.

20 To illustrate this finding, Figure 10 shows (from left) the total cloud fraction, precipitation, dust surface concentration, and
the dust burden (monthly mean) for different convection parameterizations in comparison to MODIS cloud fraction and TRMM
precipitation. In general, the model exhibits the main features of the cloud cover observations; however, the EMAC (reference
setup) model underestimates the cloud cover over the Atlantic Ocean. Over the tropical areas in Africa, B1T5 leads to more
realistic results compared to MODIS relative to B1T4 (shown in the Fig. S5 in the supplement) simulation (for this region and

25 season). Over the Ocean, B1T5 considerably underestimates the cloud cover and the precipitation rate that has limited impact
on the dust transport. Over the Caribbean sites, B1T5 overestimates the cloud cover, whereas the other schemes show better
results. On the other hand, the calculated precipitation (second column) generally shows an overestimation for all schemes
except B1T5 that shows an underestimation over the ocean. As a result of the differences in the cloud cover and precipitation
rates, the model shows a different magnitude of the dust plumes (third and fourth columns) which is more pronounced for the

30 dust burden. For the reference simulation, the dust plume extends to $60°W$ with a dust burden of 200 mg.m^{-2}, whereas for
simulation B1T3 the same dust burden is obtained at $80°W$ and westwards. The difference in the dust plume magnitude merely
results from different removal efficiencies because of different precipitation rates.

For a quantitative comparison, the average meridional dust burden in the dust outflow over the Atlantic Ocean region ($10°$–
$25°N$) for different convection parameterizations, together with the precipitation (middle panel) and the column averaged aged
dust proxy (ADP) (bottom panel), is shown in Fig. 11 which was introduced by Abdelkader et al. (2015). The ADP, which
represents the ratio between aged and non-aged dust particles, indicates the level of dust aging (the mass fraction of the aged to
the total dust mass). A zero ADP value indicates no aged dust particles ("pristine" or freshly emitted particles in the insoluble

5 mode), whereas a value of one indicates that all dust particles are considered to be aged (all particles are coated and present in the soluble dust mode).

The dust burden shows a very steep gradient westward over the Atlantic Ocean because of the dust removal by deposition (sedimentation and scavenging mechanisms) during the transport. Over the Atlantic (within DTA), the gradient is linear in the logarithmic scale, whereas the gradient is nonlinear over the Western and Eastern Atlantic (especially within DIZ). The dust

10 burden over West Africa (eastern to $10°$W) shows roughly $1000\,\mu\mathrm{g\,m^{-3}}$ and declines to $50\,\mu\mathrm{g\,m^{-3}}$ over the Caribbean. The different parameterization schemes show more than a factor of 2 difference between the dust burden over Western Africa and a factor of 3 over the Caribbean. This is primarily a result of different precipitation rates and different associated dust removal. The two precipitation peaks (over Western Africa and the Caribbean), as shown in Fig. 5, can also be seen in Fig. 11, but to a lesser extent because the averaging is performed over a wider area (dust plume) that is not associated with precipitation. The

15 higher precipitation rate over the western and eastern parts of the Atlantic results in an enhanced dust scavenging. Over the Atlantic, the precipitation is lower and therefore the removal by sedimentation is relatively stronger ($\approx 2\,\mathrm{g\,m^{-2}}$ compared to $\approx 0.2\,\mathrm{g\,m^{-2}}$ during July 2009), whereas the elevated precipitation over the Caribbean shows the maximum dust deposition due to scavenging. As a result, the dust burden is an order of magnitude lower over the Caribbean compared with West Africa. In addition, there is a clear anticorrelation between the dust burden and the precipitation amount over both sides of the Atlantic.

20 The comparison of precipitation with TRMM observations shows that the EMAC model gives more realistic results over West Africa compared with the Caribbean for all convection schemes.

The ADP (Fig. 11) illustrates the effect of convection schemes on the transatlantic dust transport and shows the highest sensitivity for the convection parameterization. Over West Africa, the dust is aged with ADP values between 0.2 and 0.4, whereas over the Caribbean the ADP values are higher ranging between 0.3 and 0.5. The lower ADP values over West Africa

25 indicate the higher dust loadings, which require a larger amount of condensable material to age. Over the Caribbean, the dust loading is much lower due to removal during the transport which is about 5 days, for instance Gläser et al. (2015), long enough for coating by acids and other soluble materials which cause the dust to become more aged (ADP = 0.6) compared to the Western African side (ADP=0.35). The high precipitation amount at $15°$W over the Western Africa region results in higher scavenging of the aged dust particles compared with the "pristine" (nonaged) dust particles and results in a decrease in

30 the ADP values that are in agreement with the results of Abdelkader et al. (2015). Western to $15°$W, the dust is transported over the Atlantic at a region where the precipitation is lower (middle panels). This results in an increase in the aging levels. Consequently, the EMAC reference simulation (with higher precipitation) shows higher ADP (0.35 compared to 0.2) values as a result of the lower dust burden, which is caused by too efficient wet removal.

The convection sensitivity analysis indicates a very strong removal of the dust during transatlantic transport with the EMAC default convection scheme, which is indicated by the underestimation of the AOD over the Caribbean. In addition, the level of dust aging controls the efficiency of dust scavenging. Higher levels of aged dust and higher precipitation amounts significantly decrease the dust burden and thus the AOD over the Caribbean. This suggests that improving the transatlantic dust transports requires improved convection parameterization and more realistic precipitation rates in parallel with the improved dust aging.

Atmospheric
Chemistry
and Physics
Discussions

4.3 Dust chemical aging

The level of dust aging depends on the availability of inorganic acids, i.e., volatile and semivolatile compounds. To further investigate the impact of the dust aging on the transatlantic dust transport, dust aging was excluded for an additional sensitivity study. For this case, the condensation of acids on insoluble dust particles is excluded, which suppresses water uptake by dust particles. Figure 12 shows the AOD time series at the AERONET stations on both sides of the Atlantic for two cases, i.e., "Aging" and "No Aging". Generally, the "Aging" case systematically shows a higher AOD as compared with the "No Aging" case, which emphasizes the importance of this process and the associated water uptake in agreement with the results of Pozzer et al. (2015). The dust aging has a stronger impact on the AOD over Western Africa, especially at the Capo Verde and Dakar stations during the two dust outbreaks discussed above. The Aging case shows about 0.2 higher AOD compared with the "No Aging" case as a result of the larger particle size and the associated water uptake. This increases the scattering cross section and thus the AOD. Over the Caribbean, the dust aging shows a smaller impact on the AOD; the "Aging" case shows only about 0.05 higher AOD because of the lower contribution of the dust to the overall AOD values (which includes the contribution of other aerosol species, sea salt, etc., for instance). During the high dust outbreaks, the concentration of the soluble compounds required to coat such a large amount of dust is not available according to the EMAC model. The aged dust particles are removed more efficiently during transport and relatively more uncoated dust particles reach the Caribbean. As a result, the dust aging has a limited effect on the AOD over the Caribbean AERONET stations.

Figure 13 shows the regional difference (monthly mean) for (a) the dust burden, (b) AOD, (c) dust emissions averaged over the region from $18°$-$22°$N, and (d) the dust-only AOD ("No Aging" minus "Aging" case). The results show a higher dust burden over the dust source regions in Western Africa for the "No Aging" case as compared with the reference case ("Aging" case). For the "No Aging" case, the dust plume is slightly extended further to the west over the Caribbean because of the lower dust removal during transport. The difference between the two simulations decreases during the transport, which is supported by the differences in the dust-only AOD. In contrast, the difference in the total AOD shows lower AOD values over the dust source region compared with the "Aging" case, which indicates a significant contribution of the dust aging to the total AOD. Interestingly, the negative feedback between the AOD and the radiation scheme results in higher dust emission over the region from $10°$E to $0°$ and thus causes a higher dust burden. The average dust emission during July 2009 over the region from $18°$N to $22°$N (lower panel) shows that the dust emission for the "Aging" case is on average higher by about $3\,\mathrm{g\,m^{-2}}$, which results in a higher dust burden by $1\,\mathrm{g\,m^{-2}}$ while the remaining amount of the dust ($2\,\mathrm{g\,m^{-3}}$) is deposited. The higher AOD in the "Aging" case results in stronger scattering of short-wave solar radiation, lower surface radiation fluxes but higher surface wind speed (as shown in Fig. S7 in the supplement), and eventually stronger dust emission of $2\,\mathrm{g\,m^{-2}}$. The increased wind speed (more than $0.25\,\mathrm{m\,s^{-1}}$ on monthly average) could result either from the increase in the surface temperature because of the absorption of the dust particles and the resultant increase in the surface pressure (Menon, 2002; Mishra et al., 2014) or from a change in the horizontal temperature gradient that also increases the local wind speed (Rémy et al., 2015). On the other hand, the more efficient removal of the large dust particles in the "Aging" case by both scavenging and sedimentation results in lower dust burden and thus the lower AOD. The balance between the two competing processes defines the impact of dust aging on AOD.

5   The difference in the dust-only optical depth is shown in the lower right panel of Fig. 13 and indicates that the "No Aging"
    case has higher dust optical depth as a result of the lower dust removal as compared with the "Aging" case. The difference is at
    a minimum within a region between 18°N to 22°N. However, the total AOD shows that the "No Aging" case leads to a lower
    AOD, which is significant over Western Africa and less pronounced over the Caribbean sites. Note that the AOD, as compared
    with AERONET stations, shown in Fig. 12 does not resolve this large difference because the AERONET stations are all located
10 in the DTA region where the differences are obviously lower.

    The substantial higher AOD for the "Aging" case (0.3 on a monthly mean basis) primarily results from the dust aging
    because of the associated water uptake. Figure 14 shows the monthly averaged burden for lumped gas-phase acids (sum of
    $HCl+HNO_3+H_2SO_4$) and the difference between both simulations. The figure also shows the corresponding lumped inorganic
    aerosol mass (sum of $SO_4^{2-} + HSO_4^- + NO_3^- + NH_4^+ + Cl^- + Na^+ + Ca^{2+} + K^+ + Mg^{2+}$) and the aerosol associated water mass.
15 For the "Aging" case, the burden of the lumped acids is very low over the dust source region because of the uptake by dust
    particles – an important effect which has been also recently studied with the EMAC model by Karydis et al. (2016) for the nitric
    acid uptake. Consequently, the burden of the lumped aerosols is higher over the dust source region and over the dust outflow
    region, because of the additional neutralization of the calcium ions by anions and the associated absorption of water vapor by
    the resulting calcium salts. As a result, the aerosol-associated water increases by more than $255 \, \mathrm{mg \, m^{-2}}$ for the aged case. The
20 effect of dust aging is a result of the gas–aerosol partitioning that clearly affects the AOD. It is best observed in the differences
    (right column of Figure 14). This shows that the impact of the dust aging can be very high, mainly due to the associated uptake
    of aerosol water. We refer to this effect as the "direct effect of dust aging." In addition, we refer to the higher removal of aged
    dust (by both sedimentation and scavenging), and the consequently shorter dust lifetime, as the "indirect effect of dust aging"
    – both effects are introduced in this study.

25 To obtain better statistics for the effect of dust aging, the same analysis ("Aging" versus "No Aging") was applied to the
    entire evaluation period (2000–2012) at lower model resolution (i.e., T42, or $\approx 280 \, \mathrm{km}$). Figure 15 shows the long-term
    meridional dust burden mean and the model precipitation for TRMM observations over the DTA and DIR zones (as discussed
    above). The "No Aging" case consistently shows higher dust burden in the DIR zone as a result of more efficient scavenging
    for the "Aging" case. Even for this long-term average, the dust burden is three times higher for the "No Aging" case than the
30 "Aging" case over the Caribbean sites. However, the impact of scavenging of the "Aging" case is higher in the region between
    10°W and 20°W, which corresponds with the high precipitation peak in the Western Africa region.

5   Conclusions

Tansatlantic dust transport is a major large-scale atmospheric phenomenon. Although the EMAC model mostly reproduces the
dust pattern during the transatlantic dust transport, the dust loadings and AOD can deviate in magnitude and seasonality from
observations. To examine different key processes, the dust outflow region has been divided into two subregions: (1) the dust-
ITCZ (DIZ) zone and (2) the adjacent dust transport over the Atlantic Ocean (DTA) zone. In the former, the dust is removed
5   primarily by scavenging, whereas in the latter region sedimentation is predominant. Considering the two subregions allows the

distinction of factors that affect the transatlantic dust transport. Several sensitivity studies were conducted using the EMAC model reference setup that was implemented by Abdelkader et al. (2015), which uses an online dust emission scheme and explicit dust chemical aging. The modeled AOD is sensitive to the emission flux parameterization but it is even more sensitive to the choice of the convection scheme. The modeled AOD is more sensitive to the dust emission flux over West Africa

10　compared with the Caribbean sites. EMAC can use several convection schemes, and the dust outflow to the Caribbean best represented if the ECMWF convection scheme is used – mainly because the precipitation within the ITCZ is better reproduced compared to the other schemes (available in EMAC). As a result of the more realistic precipitation, the AOD on both sides of the Atlantic Ocean is significantly improved, which is largely controlled by wet removal processes within the DIZ zone, especially when dust aging is considered.

15　Dust aging changes the particle sizes because of the additional amount of condensed inorganic acids and the associated uptake of water vapor by the neutralization products (salts). Therefore, the aged dust particles are larger and scatter more light, whereas they are more efficiently removed by dry and wet removal processes. To distinguish these effects, we introduce the *"direct effect of dust aging"* and the *"indirect effect of dust aging"*. These effects clearly show the differences between the "Aging" and " No Aging" simulations, and the result of the air-pollution–dust interactions that can regionally strongly influence

20　the AOD. Dust aging has the largest impact on the AOD over West Africa and on the dust burden in the ITCZ. The higher impact on the AOD results from the increase in the aerosol burden (more than $120\,\mathrm{mg\,m^{-2}}$) due to the uptake of acids and associated water by the originally insoluble dust particles. This directly increases the AOD by 0.15 on monthly average. As a result of the radiative feedback on the atmospheric dynamics and circulation, the dust emission regionally increases. On the other hand, the aged dust particles are more efficiently removed in our EMAC reference setup compared with the "non-aged"

25　dust particles case. The enhanced removal of aged particles decreases the dust burden and lifetime, indirectly affecting the AOD. Both processes are significant and the net effect depends on the region and the level of dust aging, which is controlled by the strength of the dust outflow and the collocated air-pollution levels.

Appendix A: Evaluation metrics

- RMSE – Root Mean Square Error between the model (m) and the observations (o):

30
$$RMSE = \sqrt{\frac{1}{N}\sum (X_m - X_o)^2} \tag{A1}$$

- σ – Standard deviation of the model (σ_m) and the observation (σ_o) for variable (X_i) with average of ($\bar{X}$) with N the number of observations:

$$\sigma = \sqrt{\frac{1}{N}\sum_{i=1}^{N}(X_i - \bar{X})^2}, \qquad where \quad \bar{X} = \frac{1}{N}\sum_{i=1}^{N}X_i \tag{A2}$$

- R – Correlation coefficient between the model (m) and the observations (o):

$$R = \frac{\sum_{i=1}^{N}(X_i^m - \bar{X^m})(X_i^o - \bar{X^o})}{\sum_{i=1}^{N}(X_i^m - \bar{X^m})^2 \sum_{i=1}^{N}(X_i^o - \bar{X^o})^2} \tag{A3}$$

Atmospheric
Chemistry
and Physics
Discussions

Open Access

5   – MBE – Mean Bias Error between the model and the observations:

$$MBE = \frac{1}{N} \sum (X_m - X_o) \tag{A4}$$

   – SS1 – Skill score between the model (m) and the observations (o) (Taylor, 2001):

$$SS1 = \frac{4(1+R)}{(\sigma_f + 1/\sigma_f)^2(1+R_0)}, \qquad where \quad \sigma_f = \frac{\sigma_o}{\sigma_m} \quad R_0 = 0.0 \tag{A5}$$

Atmospheric
Chemistry
and Physics
Discussions

References

Abdelkader, M., Metzger, S., Mamouri, R. E., Astitha, M., Barrie, L., Levin, Z., and Lelieveld, J.: Dust–air pollution dynamics over the eastern Mediterranean, Atmospheric Chemistry and Physics, 15, 9173–9189, doi:10.5194/acp-15-9173-2015, http://www.atmos-chem-phys.net/15/9173/2015/, 2015.

Abouchami, W., Näthe, K., Kumar, A., Galer, S. J., Jochum, K. P., Williams, E., Horbe, A. M., Rosa, J. W., Balsam, W., Adams, D., Mezger, K., and Andreae, M. O.: Geochemical and isotopic characterization of the Bodélé Depression dust source and implications for transatlantic dust transport to the Amazon Basin, Earth and Planetary Science Letters, 380, 112–123, doi:10.1016/j.epsl.2013.08.028, http://linkinghub.elsevier.com/retrieve/pii/S0012821X13004652, 2013.

Adams, A. M., Prospero, J. M., and Zhang, C.: CALIPSO-Derived Three-Dimensional Structure of Aerosol over the Atlantic Basin and Adjacent Continents, Journal of Climate, 25, 6862–6879, doi:10.1175/JCLI-D-11-00672.1, http://journals.ametsoc.org/doi/abs/10.1175/JCLI-D-11-00672.1, 2012.

Alexander, J. M., Grassian, V. H., Young, M. A., and Kleiber, P. D.: Optical properties of selected components of mineral dust aerosol processed with organic acids and humic material: Optical Properties of Mineral Dust, Journal of Geophysical Research: Atmospheres, 120, 2437–2452, doi:10.1002/2014JD022782, http://doi.wiley.com/10.1002/2014JD022782, 2015.

Alizadeh-Choobari, O., Sturman, A., and Zawar-Reza, P.: A global satellite view of the seasonal distribution of mineral dust and its correlation with atmospheric circulation, Dynamics of Atmospheres and Oceans, 68, 20–34, doi:10.1016/j.dynatmoce.2014.07.002, http://linkinghub.elsevier.com/retrieve/pii/S0377026514000347, 2014.

Astitha, M., Kallos, G., Spyrou, C., O'Hirok, W., Lelieveld, J., and Denier van der Gon, H. A. C.: Modelling the chemically aged and mixed aerosols over the eastern central Atlantic Ocean – potential impacts, Atmospheric Chemistry and Physics, 10, 5797–5822, doi:10.5194/acp-10-5797-2010, http://www.atmos-chem-phys.net/10/5797/2010/, 2010.

Astitha, M., Lelieveld, J., Abdel Kader, M., Pozzer, A., and de Meij, A.: Parameterization of dust emissions in the global atmospheric chemistry-climate model EMAC: impact of nudging and soil properties, Atmospheric Chemistry and Physics, 12, 11 057–11 083, doi:10.5194/acp-12-11057-2012, http://www.atmos-chem-phys.net/12/11057/2012/, 2012.

Baker, A. R., Lesworth, T., Adams, C., Jickells, T. D., and Ganzeveld, L.: Estimation of atmospheric nutrient inputs to the Atlantic Ocean from 50°N to 50°S based on large-scale field sampling: Fixed nitrogen and dry deposition of phosphorus: ATLANTIC ATMO-SPHERIC NUTRIENT INPUTS, Global Biogeochemical Cycles, 24, n/a–n/a, doi:10.1029/2009GB003634, http://doi.wiley.com/10.1029/2009GB003634, 2010.

Baker, A. R., Adams, C., Bell, T. G., Jickells, T. D., and Ganzeveld, L.: Estimation of atmospheric nutrient inputs to the Atlantic Ocean from 50°N to 50°S based on large-scale field sampling: Iron and other dust-associated elements: ATLANTIC ATMOSPHERIC IRON INPUTS, Global Biogeochemical Cycles, 27, 755–767, doi:10.1002/gbc.20062, http://doi.wiley.com/10.1002/gbc.20062, 2013.

Bangalath, H. K. and Stenchikov, G.: Role of dust direct radiative effect on the tropical rain belt over Middle East and North Africa: A high-resolution AGCM study: DUST RADIATIVE EFFECT OVER MENA, Journal of Geophysical Research: Atmospheres, 120, 4564–4584, doi:10.1002/2015JD023122, http://doi.wiley.com/10.1002/2015JD023122, 2015.

Bechtold, P., Chaboureau, J.-P., Beljaars, A., Betts, A. K., Köhler, M., Miller, M., and Redelsperger, J.-L.: The simulation of the diurnal cycle of convective precipitation over land in a global model, Quarterly Journal of the Royal Meteorological Society, 130, 3119–3137, doi:10.1256/qj.03.103, http://dx.doi.org/10.1256/qj.03.103, 2004.

Atmospheric
Chemistry
and Physics
Discussions

Open Access

Ben-Ami, Y., Koren, I., and Altaratz, O.: Patterns of North African dust transport over the Atlantic: winter vs. summer, based on CALIPSO first year data, Atmospheric Chemistry and Physics, 9, 7867–7875, doi:10.5194/acp-9-7867-2009, http://www.atmos-chem-phys.net/9/7867/2009/, 2009.

Ben-Ami, Y., Koren, I., Rudich, Y., Artaxo, P., Martin, S. T., and Andreae, M. O.: Transport of North African dust from the Bodélé depression to the Amazon Basin: a case study, Atmospheric Chemistry and Physics, 10, 7533–7544, doi:10.5194/acp-10-7533-2010, http://www.atmos-chem-phys.net/10/7533/2010/, 2010.

Ben-Ami, Y., Koren, I., Altaratz, O., Kostinski, A., and Lehahn, Y.: Discernible rhythm in the spatio/temporal distributions of transatlantic dust, Atmospheric Chemistry and Physics, 12, 2253–2262, doi:10.5194/acp-12-2253-2012, http://www.atmos-chem-phys.net/12/2253/2012/, 2012.

Bristow, C. S., Hudson-Edwards, K. A., and Chappell, A.: Fertilizing the Amazon and equatorial Atlantic with West African dust: AFRICAN FERTILIZER FOR AMAZON AND ATLANTIC, Geophysical Research Letters, 37, n/a–n/a, doi:10.1029/2010GL043486, http://doi.wiley.com/10.1029/2010GL043486, 2010.

Chin, M., Diehl, T., Tan, Q., Prospero, J. M., Kahn, R. A., Remer, L. A., Yu, H., Sayer, A. M., Bian, H., Geogdzhayev, I. V., Holben, B. N., Howell, S. G., Huebert, B. J., Hsu, N. C., Kim, D., Kucsera, T. L., Levy, R. C., Mishchenko, M. I., Pan, X., Quinn, P. K., Schuster, G. L., Streets, D. G., Strode, S. A., Torres, O., and Zhao, X.-P.: Multi-decadal aerosol variations from 1980 to 2009: a perspective from observations and a global model, Atmospheric Chemistry and Physics, 14, 3657–3690, doi:10.5194/acp-14-3657-2014, http://www.atmos-chem-phys.net/14/3657/2014/, 2014.

Cuevas, E., Camino, C., Benedetti, A., Basart, S., Terradellas, E., Baldasano, J. M., Morcrette, J. J., Marticorena, B., Goloub, P., Mortier, A., Berjón, A., Hernández, Y., Gil-Ojeda, M., and Schulz, M.: The MACC-II 2007–2008 reanalysis: atmospheric dust evaluation and characterization over northern Africa and the Middle East, Atmospheric Chemistry and Physics, 15, 3991–4024, doi:10.5194/acp-15-3991-2015, http://www.atmos-chem-phys.net/15/3991/2015/, 2015.

Darmenova, K., Sokolik, I. N., Shao, Y., Marticorena, B., and Bergametti, G.: Development of a physically based dust emission module within the Weather Research and Forecasting (WRF) model: Assessment of dust emission parameterizations and input parameters for source regions in Central and East Asia, Journal of Geophysical Research, 114, doi:10.1029/2008JD011236, http://www.agu.org/pubs/crossref/2009/2008JD011236.shtml, 2009.

Diner, D., Beckert, J., Reilly, T., Bruegge, C., Conel, J., Kahn, R., Martonchik, J., Ackerman, T., Davies, R., Gerstl, S., Gordon, H., Muller, J., Myneni, R., Sellers, P., Pinty, B., and Verstraete, M.: Multi-angle Imaging SpectroRadiometer (MISR) instrument description and experiment overview, IEEE Transactions on Geoscience and Remote Sensing, 36, 1072–1087, doi:10.1109/36.700992, http://ieeexplore.ieee.org/lpdocs/epic03/wrapper.htm?arnumber=700992, 1998.

Doherty, O. M., Riemer, N., and Hameed, S.: Control of Saharan mineral dust transport to Barbados in winter by the Intertropical Convergence Zone over West Africa, Journal of Geophysical Research: Atmospheres, 117, n/a–n/a, doi:10.1029/2012JD017767, http://dx.doi.org/10.1029/2012JD017767, 2012.

Doherty, O. M., Riemer, N., and Hameed, S.: Role of the convergence zone over West Africa in controlling Saharan mineral dust load and transport in the boreal summer, Tellus B, 66, doi:10.3402/tellusb.v66.23191, http://www.tellusb.net/index.php/tellusb/article/view/23191, 2014.

Fountoukis, C. and Nenes, A.: ISORROPIA II: a computationally efficient thermodynamic equilibrium model for K^+ - Ca^{2+} - Mg^{2+} - NH_4^+ - Na^+ - SO_4^{2-} - NO_3^- - Cl^- - H_2O aerosols, Atmos. Chem. Phys., 7, 4639–4659, doi:10.5194/acp-7-4639-2007, http://www.atmos-chem-phys.net/7/4639/2007/, 2007.

Ginoux, P., Prospero, J., Torres, O., and Chin, M.: Long-term simulation of global dust distribution with the GOCART model: correlation with North Atlantic Oscillation, Environmental Modelling & Software, 19, 113–128, doi:10.1016/S1364-8152(03)00114-2, http://linkinghub. elsevier.com/retrieve/pii/S1364815203001142, 2004.

Gläser, G., Wernli, H., Kerkweg, A., and Teubler, F.: The transatlantic dust transport from North Africa to the Americas-Its characteristics and source regions: TRANSATLANTIC DUST TRANSPORT, Journal of Geophysical Research: Atmospheres, 120, 11,231–11,252, doi:10.1002/2015JD023792, http://doi.wiley.com/10.1002/2015JD023792, 2015.

Grant, A. L. M. and Brown, A. R.: A similarity hypothesis for shallow-cumulus transports, Quarterly Journal of the Royal Meteorological Society, 125, 1913–1936, doi:10.1002/qj.49712555802, http://dx.doi.org/10.1002/qj.49712555802, 1999.

Groß, S., Freudenthaler, V., Schepanski, K., Toledano, C., Schäfler, A., Ansmann, A., and Weinzierl, B.: Optical properties of long-range transported Saharan dust over Barbados as measured by dual-wavelength depolarization Raman lidar measurements, Atmospheric Chemistry and Physics, 15, 11 067–11 080, doi:10.5194/acp-15-11067-2015, http://www.atmos-chem-phys.net/15/11067/2015/, 2015.

Guo, Y., Tian, B., Kahn, R. A., Kalashnikova, O., Wong, S., and Waliser, D. E.: Tropical Atlantic dust and smoke aerosol variations related to the Madden-Julian Oscillation in MODIS and MISR observations: ATLANTIC DUST AND SMOKE, Journal of Geophysical Research: Atmospheres, 118, 4947–4963, doi:10.1002/jgrd.50409, http://doi.wiley.com/10.1002/jgrd.50409, 2013.

Hack, J. J.: Parameterization of moist convection in the National Center for Atmospheric Research community climate model (CCM2), Journal of Geophysical Research: Atmospheres, 99, 5551–5568, doi:10.1029/93JD03478, http://dx.doi.org/10.1029/93JD03478, 1994.

Holben, B., Eck, T., Slutsker, I., Tanré, D., Buis, J., Setzer, A., Vermote, E., Reagan, J., Kaufman, Y., Nakajima, T., Lavenu, F., Jankowiak, I., and Smirnov, A.: AERONET—A Federated Instrument Network and Data Archive for Aerosol Characterization, Remote Sensing of Environment, 66, 1–16, doi:10.1016/S0034-4257(98)00031-5, http://linkinghub.elsevier.com/retrieve/pii/S0034425798000315, 1998.

Hsu, N. C., Gautam, R., Sayer, A. M., Bettenhausen, C., Li, C., Jeong, M. J., Tsay, S.-C., and Holben, B. N.: Global and regional trends of aerosol optical depth over land and ocean using SeaWiFS measurements from 1997 to 2010, Atmospheric Chemistry and Physics, 12, 8037–8053, doi:10.5194/acp-12-8037-2012, http://www.atmos-chem-phys.net/12/8037/2012/, 2012.

Huang, J., Zhang, C., and Prospero, J. M.: Aerosol-Induced Large-Scale Variability in Precipitation over the Tropical Atlantic, Journal of Climate, 22, 4970–4988, doi:10.1175/2009JCLI2531.1, http://journals.ametsoc.org/doi/abs/10.1175/2009JCLI2531.1, 2009.

Huang, J., Zhang, C., and Prospero, J. M.: African dust outbreaks: A satellite perspective of temporal and spatial variability over the tropical Atlantic Ocean, Journal of Geophysical Research, 115, doi:10.1029/2009JD012516, http://doi.wiley.com/10.1029/2009JD012516, 2010.

Huneeus, N., Schulz, M., Balkanski, Y., Griesfeller, J., Prospero, J., Kinne, S., Bauer, S., Boucher, O., Chin, M., Dentener, F., Diehl, T., Easter, R., Fillmore, D., Ghan, S., Ginoux, P., Grini, A., Horowitz, L., Koch, D., Krol, M. C., Landing, W., Liu, X., Mahowald, N., Miller, R., Morcrette, J.-J., Myhre, G., Penner, J., Perlwitz, J., Stier, P., Takemura, T., and Zender, C. S.: Global dust model intercomparison in AeroCom phase I, Atmospheric Chemistry and Physics, 11, 7781–7816, doi:10.5194/acp-11-7781-2011, http://www.atmos-chem-phys. net/11/7781/2011/, 2011.

Jickells, T. D., An, Z. S., Andersen, K. K., Baker, A. R., Bergametti, G., Brooks, N., Cao, J. J., Boyd, P. W., Duce, R. A., Hunter, K. A., Kawahata, H., Kubilay, N., laRoche, J., Liss, P. S., Mahowald, N., Prospero, J. M., Ridgwell, A. J., Tegen, I., and Torres, R.: Global Iron Connections Between Desert Dust, Ocean Biogeochemistry, and Climate, Science, 308, 67–71, http://www.sciencemag.org/content/308/5718/67.abstract, 2005.

Joeckel, P., Kerkweg, A., Pozzer, A., Sander, R., Tost, H., Riede, H., Baumgaertner, A., Gromov, S., and Kern, B.: Development cycle 2 of the Modular Earth Submodel System (MESSy2), Geoscientific Model Development, 3, 717–752, doi:10.5194/gmd-3-717-2010, http://www.geosci-model-dev.net/3/717/2010/gmd-3-717-2010.html, 2010.

Karydis, V. A., Tsimpidi, A. P., Pozzer, A., Astitha, M., and Lelieveld, J.: Effects of mineral dust on global atmospheric nitrate concentrations, Atmospheric Chemistry and Physics, 16, 1491–1509, doi:10.5194/acp-16-1491-2016, http://www.atmos-chem-phys.net/16/1491/2016/, 2016.

Kaufman, Y. J.: Dust transport and deposition observed from the Terra-Moderate Resolution Imaging Spectroradiometer (MODIS) spacecraft over the Atlantic Ocean, Journal of Geophysical Research, 110, doi:10.1029/2003JD004436, http://www.agu.org/pubs/crossref/2005/2003JD004436.shtml, 2005.

Kaufman, Y. J., Tanré, D., Remer, L. A., Vermote, E. F., Chu, A., and Holben, B. N.: Operational remote sensing of tropospheric aerosol over land from EOS moderate resolution imaging spectroradiometer, Journal of Geophysical Research, 102, 17 051, doi:10.1029/96JD03988, http://doi.wiley.com/10.1029/96JD03988, 1997.

Kerkweg, A., Buchholz, J., Ganzeveld, L., Pozzer, A., Tost, H., and Jöckel, P.: Technical Note: An implementation of the dry removal processes DRY DEPosition and SEDImentation in the Modular Earth Submodel System (MESSy), Atmos. Chem. Phys., 6, 4617–4632, doi:10.5194/acp-6-4617-2006, http://www.atmos-chem-phys.net/6/4617/2006/, 2006.

Khan, B., Stenchikov, G., Weinzierl, B., Kalenderski, S., and Osipov, S.: Dust plume formation in the free troposphere and aerosol size distribution during the Saharan Mineral Dust Experiment in North Africa, Tellus B, 67, doi:10.3402/tellusb.v67.27170, http://www.tellusb.net/index.php/tellusb/article/view/27170, 2015.

Kim, D., Chin, M., Yu, H., Diehl, T., Tan, Q., Kahn, R. A., Tsigaridis, K., Bauer, S. E., Takemura, T., Pozzoli, L., Bellouin, N., Schulz, M., Peyridieu, S., Chédin, A., and Koffi, B.: Sources, sinks, and transatlantic transport of North African dust aerosol: A multimodel analysis and comparison with remote sensing data, Journal of Geophysical Research: Atmospheres, 119, 6259–6277, doi:10.1002/2013JD021099, http://doi.wiley.com/10.1002/2013JD021099, 2014.

Liu, C., Chu, B., Liu, Y., Ma, Q., Ma, J., He, H., Li, J., and Hao, J.: Effect of mineral dust on secondary organic aerosol yield and aerosol size in α-pinene/NOx photo-oxidation, Atmospheric Environment, 77, 781–789, doi:10.1016/j.atmosenv.2013.05.064, http://linkinghub.elsevier.com/retrieve/pii/S1352231013004378, 2013.

Liu, Z., Omar, A., Vaughan, M., Hair, J., Kittaka, C., Hu, Y., Powell, K., Trepte, C., Winker, D., Hostetler, C., Ferrare, R., and Pierce, R.: CALIPSO lidar observations of the optical properties of Saharan dust: A case study of long-range transport, Journal of Geophysical Research: Atmospheres, 113, D07 207, doi:10.1029/2007JD008878, http://dx.doi.org/10.1029/2007JD008878, 2008.

Mahowald, N. M.: Anthropocene changes in desert area: Sensitivity to climate model predictions, Geophysical Research Letters, 34, doi:10.1029/2007GL030472, http://doi.wiley.com/10.1029/2007GL030472, 2007.

Mahowald, N. M., Kloster, S., Engelstaedter, S., Moore, J. K., Mukhopadhyay, S., McConnell, J. R., Albani, S., Doney, S. C., Bhattacharya, A., Curran, M. A. J., Flanner, M. G., Hoffman, F. M., Lawrence, D. M., Lindsay, K., Mayewski, P. A., Neff, J., Rothenberg, D., Thomas, E., Thornton, P. E., and Zender, C. S.: Observed 20th century desert dust variability: impact on climate and biogeochemistry, Atmospheric Chemistry and Physics, 10, 10 875–10 893, doi:10.5194/acp-10-10875-2010, http://www.atmos-chem-phys.net/10/10875/2010/, 2010.

Marticorena, B. and Bergametti, G.: Modeling the atmospheric dust cycle: 1. Design of a soil-derived dust emission scheme, Journal of Geophysical Research, 100, 16 415–16 430, doi:10.1029/95JD00690, http://www.agu.org/pubs/crossref/1995/95JD00690.shtml, 1995.

Menon, S.: Climate Effects of Black Carbon Aerosols in China and India, Science, 297, 2250–2253, doi:10.1126/science.1075159, http://www.sciencemag.org/cgi/doi/10.1126/science.1075159, 2002.

Metzger, S., Mihalopoulos, N., and Lelieveld, J.: Importance of mineral cations and organics in gas-aerosol partitioning of reactive nitrogen compounds: case study based on MINOS results, Atmospheric Chemistry and Physics, 6, 2549–2567, doi:10.5194/acp-6-2549-2006, http://www.atmos-chem-phys.net/6/2549/2006/, 2006.

Mishra, A. K., Klingmueller, K., Fredj, E., Lelieveld, J., Rudich, Y., and Koren, I.: Radiative signature of absorbing aerosol over the eastern Mediterranean basin, Atmospheric Chemistry and Physics, 14, 7213–7231, doi:10.5194/acp-14-7213-2014, http://www.atmos-chem-phys.net/14/7213/2014/, 2014.

Möhler, O., Benz, S., Saathoff, H., Schnaiter, M., Wagner, R., Schneider, J., Walter, S., Ebert, V., and Wagner, S.: The effect of organic coating on the heterogeneous ice nucleation efficiency of mineral dust aerosols, Environmental Research Letters, 3, 025 007, doi:10.1088/1748-9326/3/2/025007, http://stacks.iop.org/1748-9326/3/i=2/a=025007?key=crossref.d9430010506fa5292539821f7ee92ca3, 2008.

Muhs, D. R., Budahn, J. R., Prospero, J. M., and Carey, S. N.: Geochemical evidence for African dust inputs to soils of western Atlantic islands: Barbados, the Bahamas, and Florida, Journal of Geophysical Research, 112, doi:10.1029/2005JF000445, http://doi.wiley.com/10.1029/2005JF000445, 2007.

Muhs, D. R., Budahn, J. R., Prospero, J. M., Skipp, G., and Herwitz, S. R.: Soil genesis on the island of Bermuda in the Quaternary: The importance of African dust transport and deposition, Journal of Geophysical Research, 117, doi:10.1029/2012JF002366, http://doi.wiley.com/10.1029/2012JF002366, 2012.

Nenes, A., Krom, M. D., Mihalopoulos, N., Van Cappellen, P., Shi, Z., Bougiatioti, A., Zarmpas, P., and Herut, B.: Atmospheric acidification of mineral aerosols: a source of bioavailable phosphorus for the oceans, Atmospheric Chemistry and Physics, 11, 6265–6272, doi:10.5194/acp-11-6265-2011, http://www.atmos-chem-phys.net/11/6265/2011/, 2011.

Nowottnick, E., Colarco, P., Ferrare, R., Chen, G., Ismail, S., Anderson, B., and Browell, E.: Online simulations of mineral dust aerosol distributions: Comparisons to NAMMA observations and sensitivity to dust emission parameterization, Journal of Geophysical Research, 115, doi:10.1029/2009JD012692, http://doi.wiley.com/10.1029/2009JD012692, 2010.

Pozzer, A., de Meij, A., Pringle, K. J., Tost, H., Doering, U. M., van Aardenne, J., and Lelieveld, J.: Distributions and regional budgets of aerosols and their precursors simulated with the EMAC chemistry-climate model, Atmospheric Chemistry and Physics, 12, 961–987, doi:10.5194/acp-12-961-2012, http://www.atmos-chem-phys.net/12/961/2012/, 2012.

Pozzer, A., de Meij, A., Yoon, J., Tost, H., Georgoulias, A. K., and Astitha, M.: AOD trends during 2001–2010 from observations and model simulations, Atmos. Chem. Phys., 15, 5521–5535, doi:10.5194/acp-15-5521-2015, http://www.atmos-chem-phys.net/15/5521/2015/, 2015.

Pringle, K. J., Tost, H., Metzger, S., Steil, B., Giannadaki, D., Nenes, A., Fountoukis, C., Stier, P., Vignati, E., and Lelieveld, J.: Description and evaluation of GMXe: a new aerosol submodel for global simulations (v1), Geoscientific Model Development, 3, 391–412, doi:10.5194/gmd-3-391-2010, http://www.geosci-model-dev.net/3/391/2010/, 2010.

Prospero, J. M., Landing, W. M., and Schulz, M.: African dust deposition to Florida: Temporal and spatial variability and comparisons to models, Journal of Geophysical Research, 115, doi:10.1029/2009JD012773, http://www.agu.org/pubs/crossref/2010/2009JD012773.shtml, 2010.

Prospero, J. M., Collard, F.-X., Molinié, J., and Jeannot, A.: Characterizing the annual cycle of African dust transport to the Caribbean Basin and South America and its impact on the environment and air quality: African dust transport to South America, Global Biogeochemical Cycles, 28, 757–773, doi:10.1002/2013GB004802, http://doi.wiley.com/10.1002/2013GB004802, 2014.

Rémy, S., Benedetti, A., Bozzo, A., Haiden, T., Jones, L., Razinger, M., Flemming, J., Engelen, R. J., Peuch, V. H., and Thepaut, J. N.: Feedbacks of dust and boundary layer meteorology during a dust storm in the eastern Mediterranean, Atmospheric Chemistry and Physics, 15, 12 909–12 933, doi:10.5194/acp-15-12909-2015, http://www.atmos-chem-phys.net/15/12909/2015/, 2015.

Atmospheric
Chemistry
and Physics
Discussions

Ridley, D. A., Heald, C. L., Pierce, J. R., and Evans, M. J.: Toward resolution-independent dust emissions in global models: Impacts on the seasonal and spatial distribution of dust: RESOLUTION-INDEPENDENT DUST EMISSIONS, Geophysical Research Letters, 40, 2873–2877, doi:10.1002/grl.50409, http://doi.wiley.com/10.1002/grl.50409, 2013.

Rybka, H. and Tost, H.: Uncertainties in future climate predictions due to convection parameterisations, Atmospheric Chemistry and Physics Discussions, 13, 26 893–26 931, doi:10.5194/acpd-13-26893-2013, http://www.atmos-chem-phys-discuss.net/13/26893/2013/, 2013.

5 Sander, R., Kerkweg, A., Jöckel, P., and Lelieveld, J.: Technical note: The new comprehensive atmospheric chemistry module MECCA, Atmospheric Chemistry and Physics, 5, 445–450, doi:10.5194/acp-5-445-2005, http://www.atmos-chem-phys.net/5/445/2005/, 2005.

Schlosser, C., Klar, J. K., Wake, B. D., Snow, J. T., Honey, D. J., Woodward, E. M. S., Lohan, M. C., Achterberg, E. P., and Moore, C. M.: Seasonal ITCZ migration dynamically controls the location of the (sub)tropical Atlantic biogeochemical divide, Proceedings of the National Academy of Sciences, 111, 1438–1442, doi:10.1073/pnas.1318670111, http://www.pnas.org/cgi/doi/10.1073/pnas.1318670111, 10 2014.

Schulz, M., Prospero, J. M., Baker, A. R., Dentener, F., Ickes, L., Liss, P. S., Mahowald, N. M., Nickovic, S., García-Pando, C. P., Rodríguez, S., Sarin, M., Tegen, I., and Duce, R. A.: Atmospheric Transport and Deposition of Mineral Dust to the Ocean: Implications for Research Needs, Environmental Science & Technology, 46, 10 390–10 404, doi:10.1021/es300073u, http://pubs.acs.org/doi/abs/10.1021/es300073u, 2012.

15 Shao, Y., Wyrwoll, K.-H., Chappell, A., Huang, J., Lin, Z., McTainsh, G. H., Mikami, M., Tanaka, T. Y., Wang, X., and Yoon, S.: Dust cycle: An emerging core theme in Earth system science, Aeolian Research, 2, 181–204, doi:10.1016/j.aeolia.2011.02.001, http://linkinghub.elsevier.com/retrieve/pii/S1875963711000085, 2011.

Taylor, K. E.: Summarizing multiple aspects of model performance in a single diagram, Journal of Geophysical Research, 106, 7183, doi:10.1029/2000JD900719, http://doi.wiley.com/10.1029/2000JD900719, 2001.

20 Tiedtke, M.: A Comprehensive Mass Flux Scheme for Cumulus Parameterization in Large-Scale Models, Monthly Weather Review, 117, 1779–1800, doi:10.1175/1520-0493(1989)117<1779:ACMFSF>2.0.CO;2, http://dx.doi.org/10.1175/1520-0493(1989)117<1779:ACMFSF>2.0.CO;2, 1989.

Tost, H., Jockel, P., Kerkweg, A., Sander, R., and Lelieveld, J.: Technical note: A new comprehensive SCAVenging submodel for global atmospheric chemistry modelling, Atmos. Chem. Phys., 6, 565–574, doi:10.5194/acp-6-565-2006, http://www.atmos-chem-phys.net/6/565/2006/, 2006a.

25 Tost, H., Jöckel, P., and Lelieveld, J.: Influence of different convection parameterisations in a GCM, Atmospheric Chemistry and Physics, 6, 5475–5493, doi:10.5194/acp-6-5475-2006, http://www.atmos-chem-phys.net/6/5475/2006/, 2006b.

Tost, H., Lawrence, M. G., Brühl, C., Jöckel, P., Team, T. G., and Team, T. S.-O.-D.: Uncertainties in atmospheric chemistry modelling due to convection parameterisations and subsequent scavenging, Atmos. Chem. Phys., 10, 1931–1951, doi:10.5194/acp-10-1931-2010, 30 http://www.atmos-chem-phys.net/10/1931/2010/, 2010.

Ussher, S. J., Achterberg, E. P., Powell, C., Baker, A. R., Jickells, T. D., Torres, R., and Worsfold, P. J.: Impact of atmospheric deposition on the contrasting iron biogeochemistry of the North and South Atlantic Ocean: SURFACE IRON IN THE ATLANTIC OCEAN, Global Biogeochemical Cycles, 27, 1096–1107, doi:10.1002/gbc.20056, http://doi.wiley.com/10.1002/gbc.20056, 2013.

van der Werf, G. R., Randerson, J. T., Giglio, L., Collatz, G. J., Mu, M., Kasibhatla, P. S., Morton, D. C., DeFries, R. S., Jin, Y., and van 35 Leeuwen, T. T.: Global fire emissions and the contribution of deforestation, savanna, forest, agricultural, and peat fires (1997–2009), Atmospheric Chemistry and Physics, 10, 11 707–11 735, doi:10.5194/acp-10-11707-2010, http://www.atmos-chem-phys.net/10/11707/2010/, 2010.

Wang, G., Cheng, C., Meng, J., Huang, Y., Li, J., and Ren, Y.: Field observation on secondary organic aerosols during Asian dust storm periods: Formation mechanism of oxalic acid and related compounds on dust surface, Atmospheric Environment, 113, 169–176, doi:10.1016/j.atmosenv.2015.05.013, http://linkinghub.elsevier.com/retrieve/pii/S1352231015300868, 2015.

Winker, D. M., Hunt, W. H., and McGill, M. J.: Initial performance assessment of CALIOP, Geophysical Research Letters, 34, doi:10.1029/2007GL030135, http://doi.wiley.com/10.1029/2007GL030135, 2007.

5 Winker, D. M., Vaughan, M. A., Omar, A., Hu, Y., Powell, K. A., Liu, Z., Hunt, W. H., and Young, S. A.: Overview of the CALIPSO Mission and CALIOP Data Processing Algorithms, Journal of Atmospheric and Oceanic Technology, 26, 2310–2323, doi:10.1175/2009JTECHA1281.1, http://journals.ametsoc.org/doi/abs/10.1175/2009JTECHA1281.1, 2009.

Wong, S., Dessler, A. E., Mahowald, N. M., Colarco, P. R., and da Silva, A.: Long-term variability in Saharan dust transport and its link to North Atlantic sea surface temperature: SAHARAN DUST AND SST VARIABILITY, Geophysical Research Letters, 35, n/a–n/a,

10 doi:10.1029/2007GL032297, http://doi.wiley.com/10.1029/2007GL032297, 2008.

Yu, H., Chin, M., Remer, L. A., Kleidman, R. G., Bellouin, N., Bian, H., and Diehl, T.: Variability of marine aerosol fine-mode fraction and estimates of anthropogenic aerosol component over cloud-free oceans from the Moderate Resolution Imaging Spectroradiometer (MODIS), Journal of Geophysical Research, 114, doi:10.1029/2008JD010648, http://www.agu.org/pubs/crossref/2009/2008JD010648.shtml, 2009.

15 Yu, H., Remer, L. A., Kahn, R. A., Chin, M., and Zhang, Y.: Satellite perspective of aerosol intercontinental transport: From qualitative tracking to quantitative characterization, Atmospheric Research, 124, 73–100, doi:10.1016/j.atmosres.2012.12.013, http://linkinghub.elsevier.com/retrieve/pii/S0169809513000070, 2013.

Yu, H., Chin, M., Bian, H., Yuan, T., Prospero, J. M., Omar, A. H., Remer, L. A., Winker, D. M., Yang, Y., Zhang, Y., and Zhang, Z.: Quantification of trans-Atlantic dust transport from seven-year (2007–2013) record of CALIPSO lidar measurements, Remote Sensing of

20 Environment, 159, 232–249, doi:10.1016/j.rse.2014.12.010, http://linkinghub.elsevier.com/retrieve/pii/S0034425714005021, 2015.

Zhang, G. and McFarlane, N. A.: Sensitivity of climate simulations to the parameterization of cumulus convection in the Canadian climate centre general circulation model, Atmosphere-Ocean, 33, 407–446, doi:10.1080/07055900.1995.9649539, http://dx.doi.org/10.1080/07055900.1995.9649539, 1995.

Table 1. Long-term EMAC model evaluation for the period 2000-2012 for AOD. Statistics are given for both sides of the Atlantic, based on the selected AERONET sites around Western Africa and the Caribbean (station average). The sites are shown in Figure 3 and the evaluation metrics are defined in the Appendix A.

	Western Africa	Caribbean
Mean_m	0.16 ± 0.27	0.12 ± 0.18
Mean_o	0.24 ± 0.37	0.14 ± 0.22
r_m	0.16 ± 0.27	0.12 ± 0.18
r_o	0.24 ± 0.37	0.14 ± 0.22
RMSE	0.35	0.23
R	0.61	0.43
MBE	-0.19	-0.11
GFE	-0.24	-0.12
SS1	0.73	0.70
PF2	0.59	0.81
PF10	1.00	1.00
NPOINTS	50288	15827

Atmospheric
Chemistry
and Physics
Discussions

Open Access

EGU

Table 2. Description of the transatlantic dust transport sensitivity simulations for two key-processes: (i) Emission flux (Sec. 4.1) and (ii) convection scheme (Sec. 4.2). Highlighted cases are shown in the manuscript (for all cases see the Supplement, Fig. S3–S4). The emitted dust mass during July 2009 for the reference case is $0.6133 \, \mathrm{kg \, m^{-2}}$.

	Case	Description
	EMAC	Reference simulation
	B1E1	Redistribution of dust between accumulation and coarse modes
	B1E2	As EMAC, accumulation fraction incased by a factor of 2.61
	B1E3	As EMAC, the coarse mode increased by a factor of 5.3
Emission	B1E4	As EMAC, the accumulation mode increased by a factor of 5.3
	B1E5	As EMAC, the accumulation mode increased by a factor of 10.6
	B1E6	As EMAC, the accumulation and coarse modes increased by a factor of 10.6 and 2.61 respectively
	B1E7	As EMAC, the accumulation and the coarse modes increased by a factor of 2.61
	B1E8	As EMAC, factor=2.61 in the horizontal flux
	EMAC	Reference simulation; TIEDTKE convection with NORDENG closure
	B1T2	TIEDTKE convection with TIEDTKE closure (Tiedtke, 1989)
Convection	B1T3	TIEDTKE convection with HYBRID closure (Tiedtke, 1989)
	B1T4	ECMWF operational convection scheme (Bechtold et al., 2004) with the shallow convection closure of Grant and Brown (1999)
	B1T5	ECMWF operational convection scheme (Bechtold et al., 2004)
	B1T6	Zhang-Hack-McFarlane convection scheme (Zhang and McFarlane, 1995; Hack, 1994)

Atmospheric
Chemistry
and Physics

Discussions

Open Access

EGU
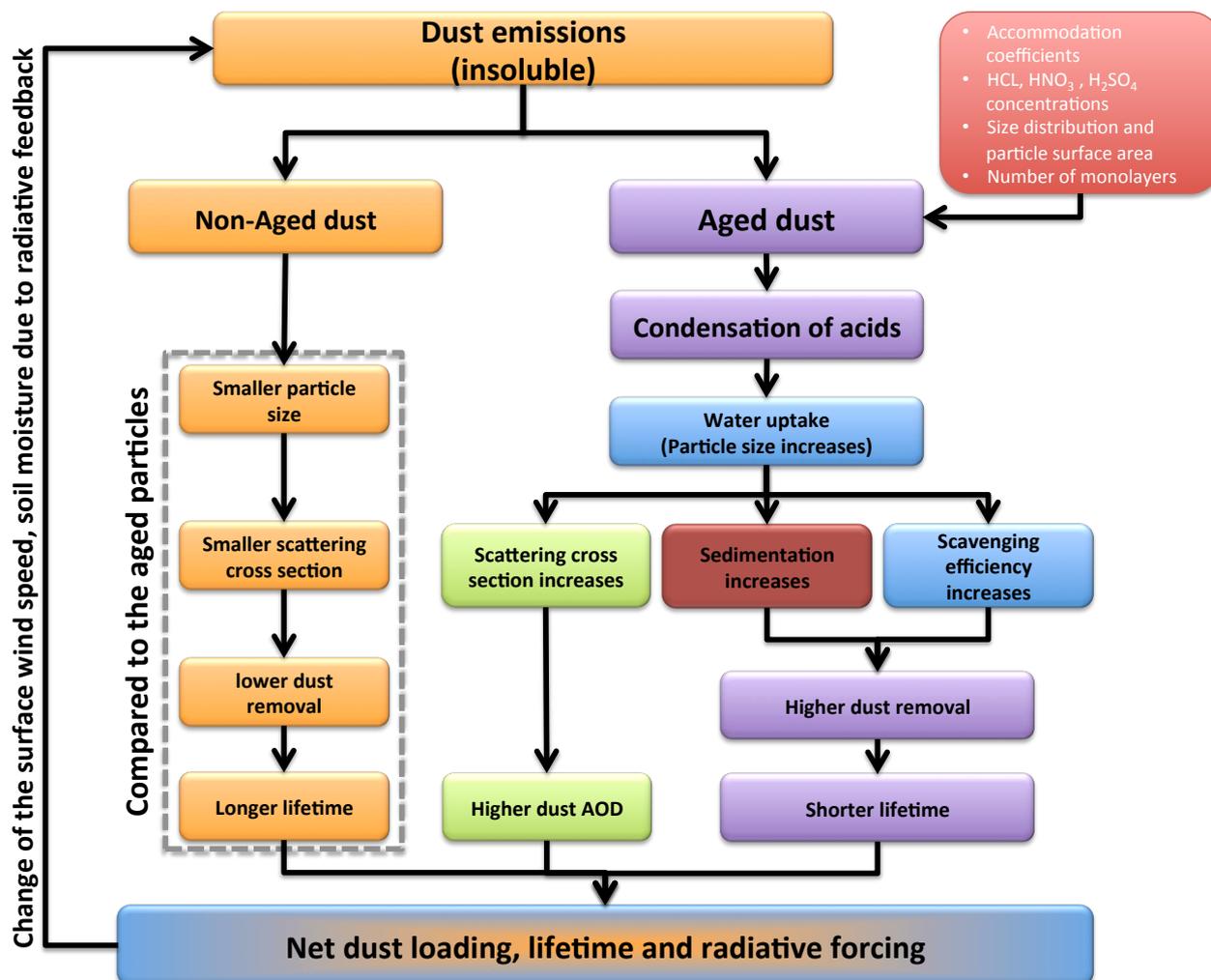
Figure 1. Schematic representation of the dust cycle and air-pollution-dust-aging-radiation feedbacks in EMAC. Air pollution controls the aging of dust particles, whereby the water uptake increases the dust particle scattering cross section, enhances the dust deposition (wet and dry) which decreases the dust lifetime. The net radiative differences between aged and non-aged dust particles are indicated.
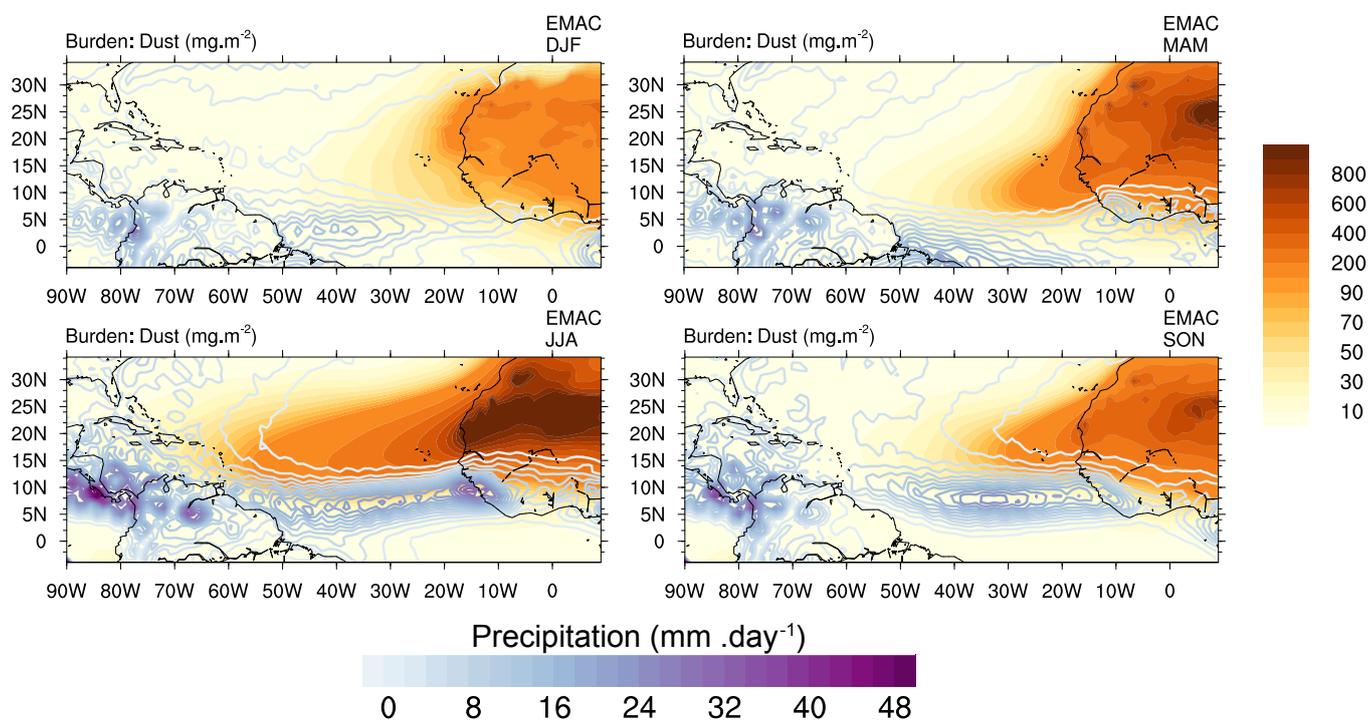
Figure 2. Seasonal averages of the dust burden and precipitation representing the transatlantic dust outflow for the entire model evaluation period (2000-2012). Dust burden and precipitation are maximum during boreal summer and minimum during winter. The orange color represent the dust burden while the purple color (contour lines) show the precipitation.

Atmospheric
Chemistry
and Physics
Discussions

Figure 3. The location of selected AERONET stations used in the transatlantic dust transport study. The upper blue line shows the approximate northern bound of the ITCZ, The yellow box shows roughly the adjacent dust transport region (DTA) zone. The region in the blue bounds represents the dust-ITCZ interaction zone (DIZ). These regions are defined according to the predominance of the dust removal mechanism shown in Fig. S1 in the supplement.

Atmospheric
Chemistry
and Physics
Discussions
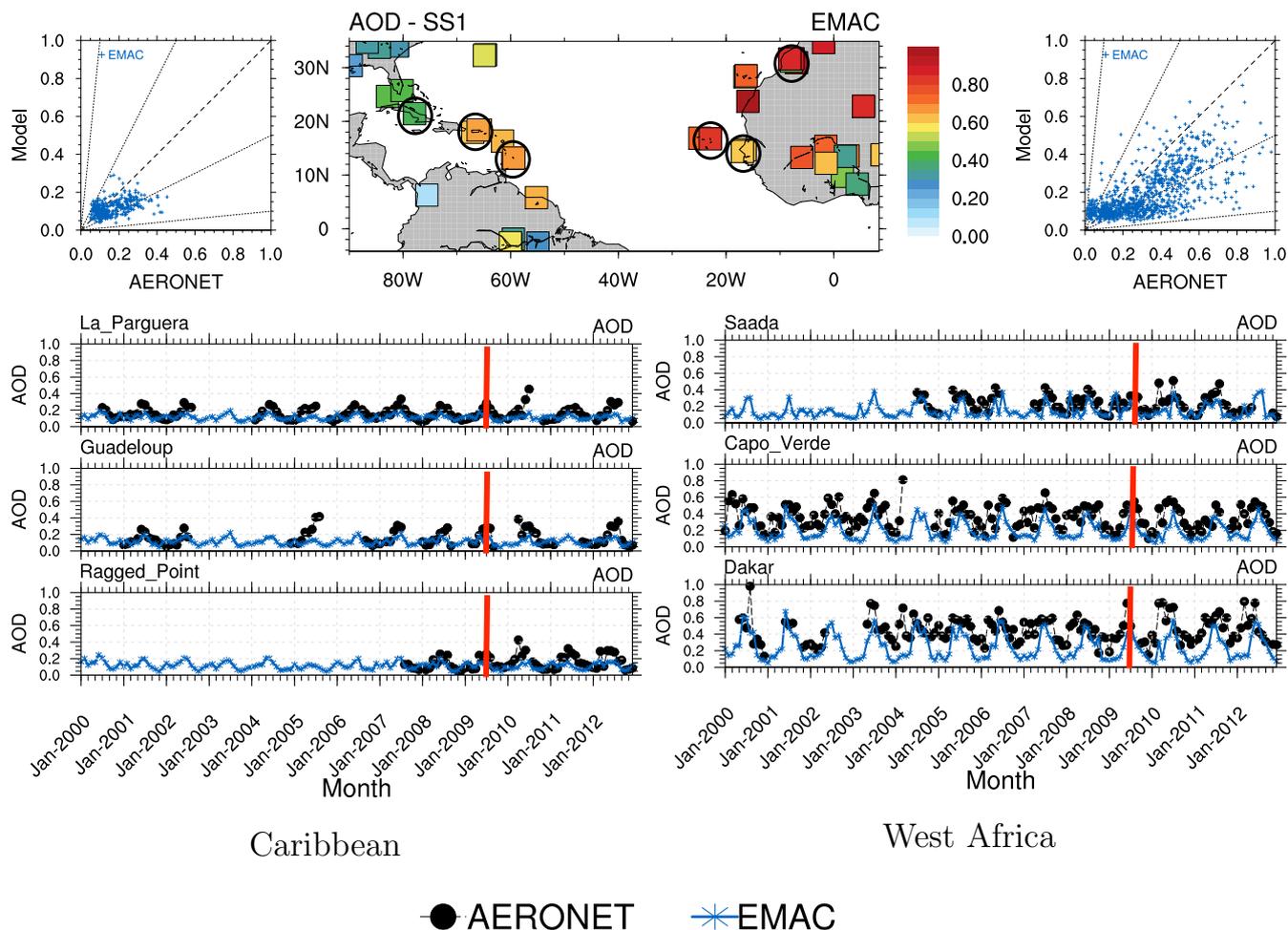
Figure 4. Long-term evaluation for AOD (2000-2012) over western Africa and the Caribbean: (Top panel) scatter plot (left for the Caribbean, right for the Western Africa region) and skill score (SS1) defined in the Appendix (A): (Lower panel) time series for stations in both regions (monthly means of 5hour averages for model and AERONET AOD). The red bars represent the July 2009 dust outflow period and the black circles show selected AERONET stations shown in Fig. 3, both are used in the sensitivity simulations.
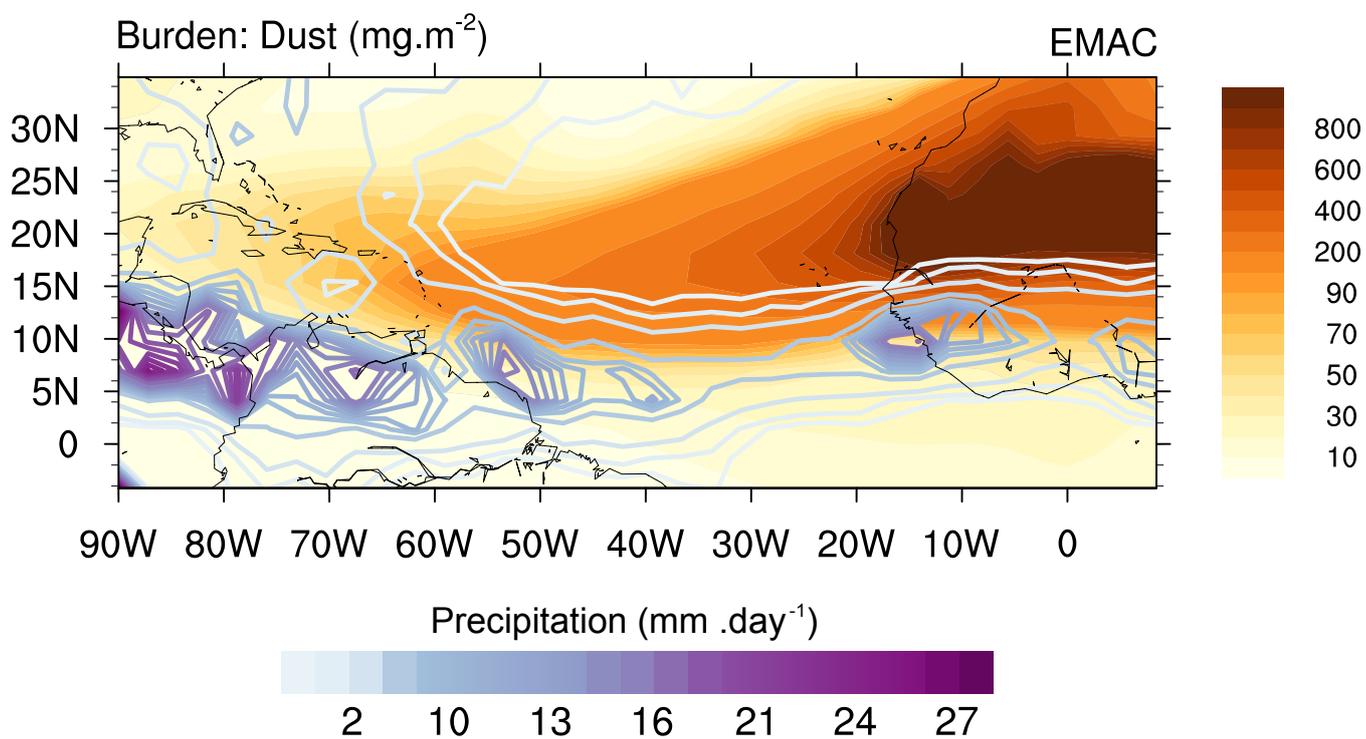
Figure 5. The EMAC computed spatial distribution of dust burden (orange) and total precipitation (purple lines) for the reference simulation for July 2009 (monthly mean). The distribution indicates the dust outflow area over the Atlantic Ocean.

Atmospheric
Chemistry
and Physics
Discussions
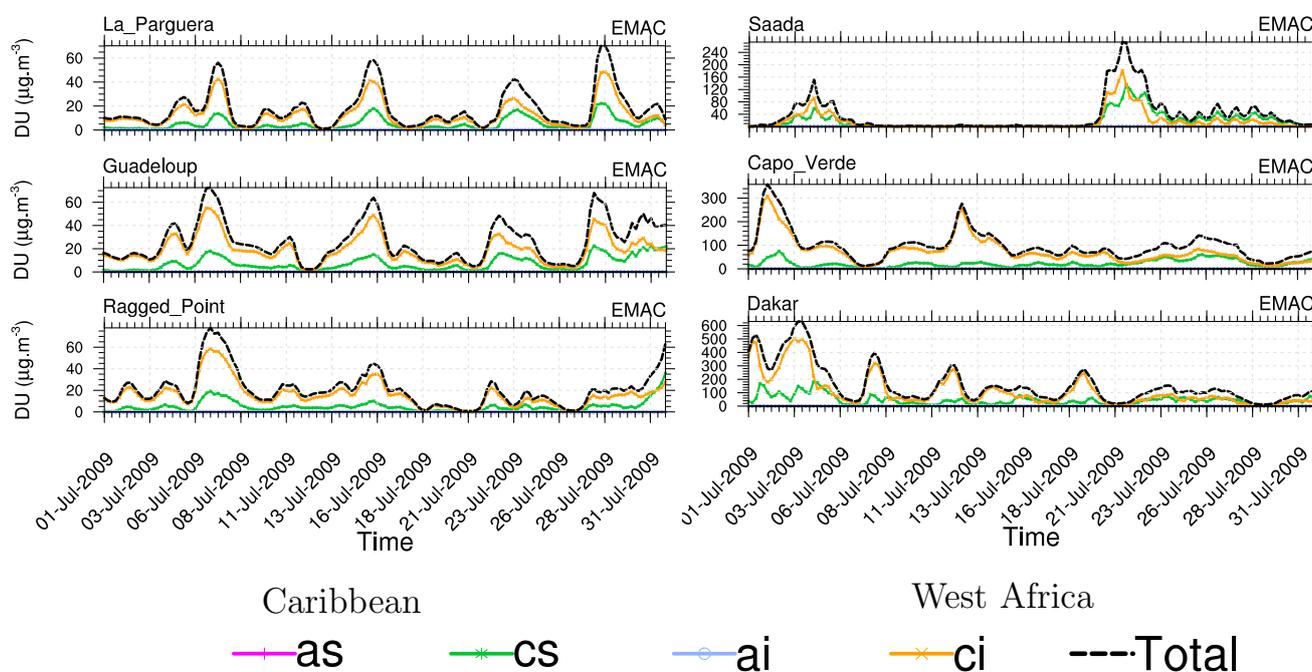
Figure 6. Time series of size-resolved surface dust concentrations for the different AERONET stations shown in Figure 3. Aerosol modes: accumulation soluble (as); coarse soluble (cs); accumulation insoluble (ai); coarse insoluble (ci). Note the different scaling which reflects the wide range of concentrations at these stations. The accumulation mode dust fraction has a much lower contribution to the total dust concentration.
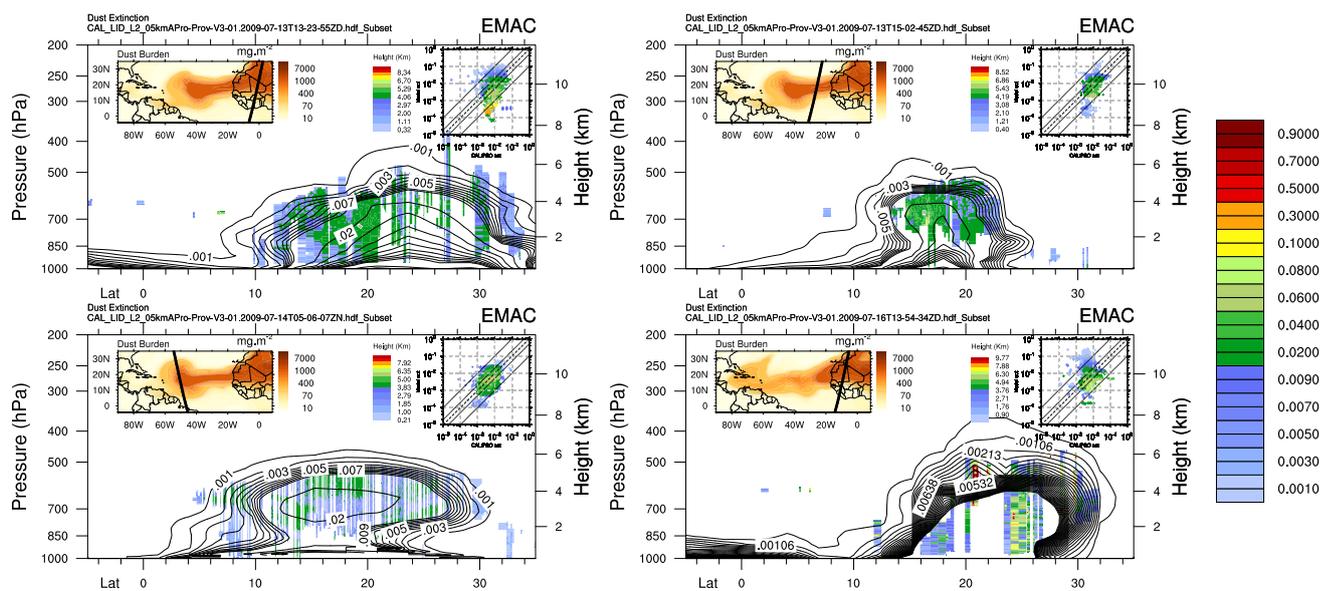
Figure 7. Collocated EMAC and CALIPSO observations of dust extinction and burden for four different CALIPSO overpasses during the second dust outbreak over the Atlantic Ocean. The time of the overpass is shown in the upper left corners (13-16th July 2009). The solid lines show the modeled and the colored contours the CALIPSO extinction, which are complemented by the scatter plots for point-to-point comparison colored by the corresponding elevations of each observation (distinguished by the colors). The lines in the scatter plots show the one-by-one line, the factor, of two and of ten. All available comparisons with CALIPSO overpasses for this period are shown in the Supplement (Fig. S2a – Fig. S2e).

Atmospheric
Chemistry
and Physics
Discussions
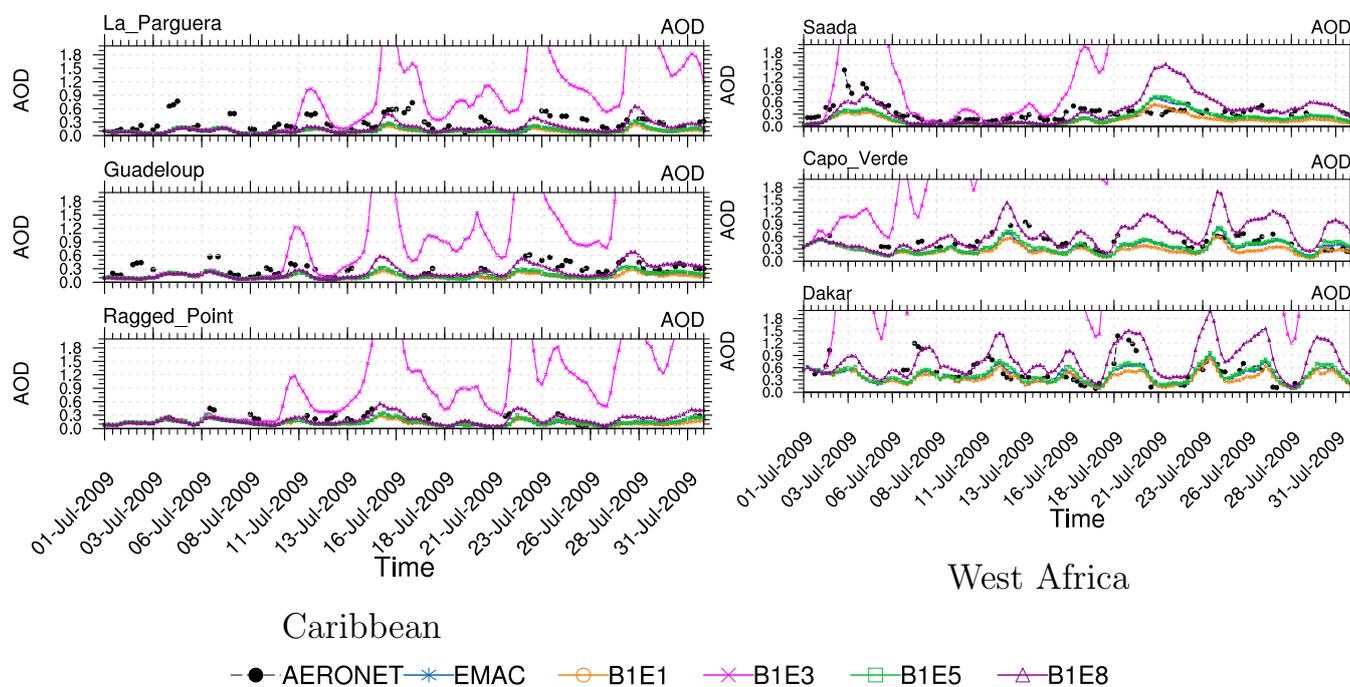
Figure 8. EMAC and AERONET AOD for the western Africa (right) and Caribbean (right) sites based on different dust emissions (Table 2).
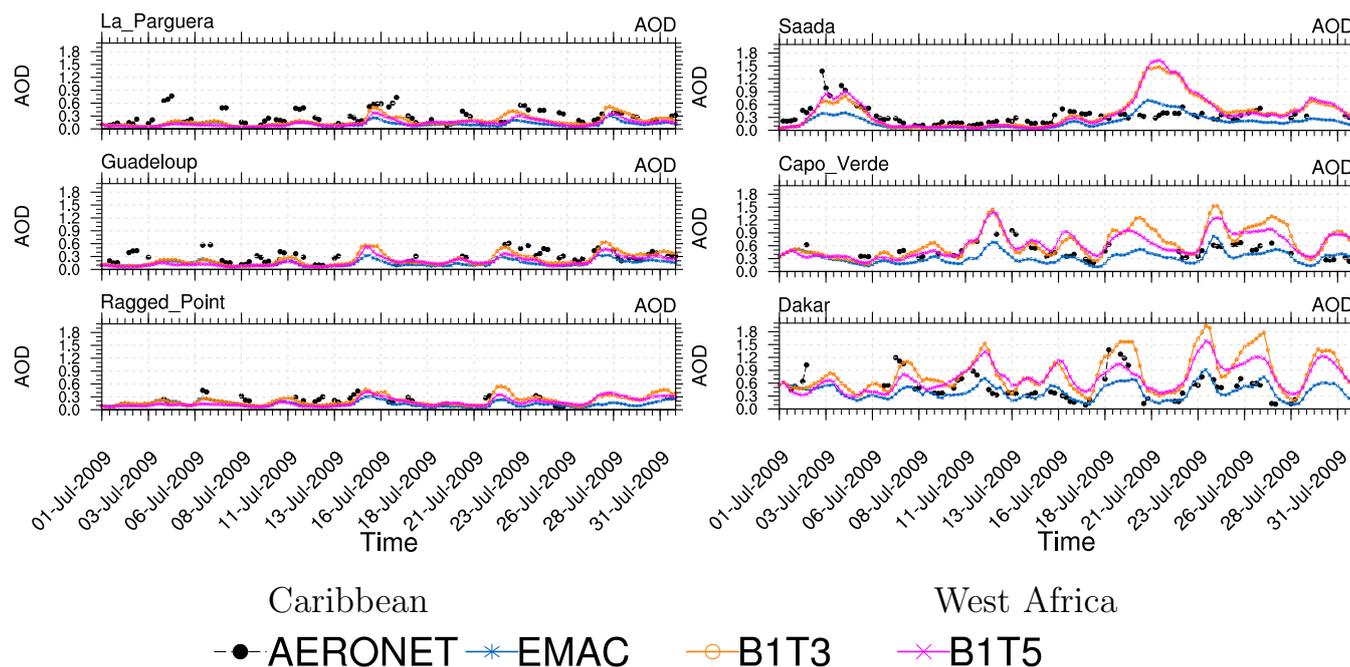
**Figure 9.** EMAC and AERONET AOD for the western Africa (right) and Caribbean (right) based on different convection schemes (Table 2).

Atmospheric
Chemistry
and Physics
Discussions

Open Access

EGU
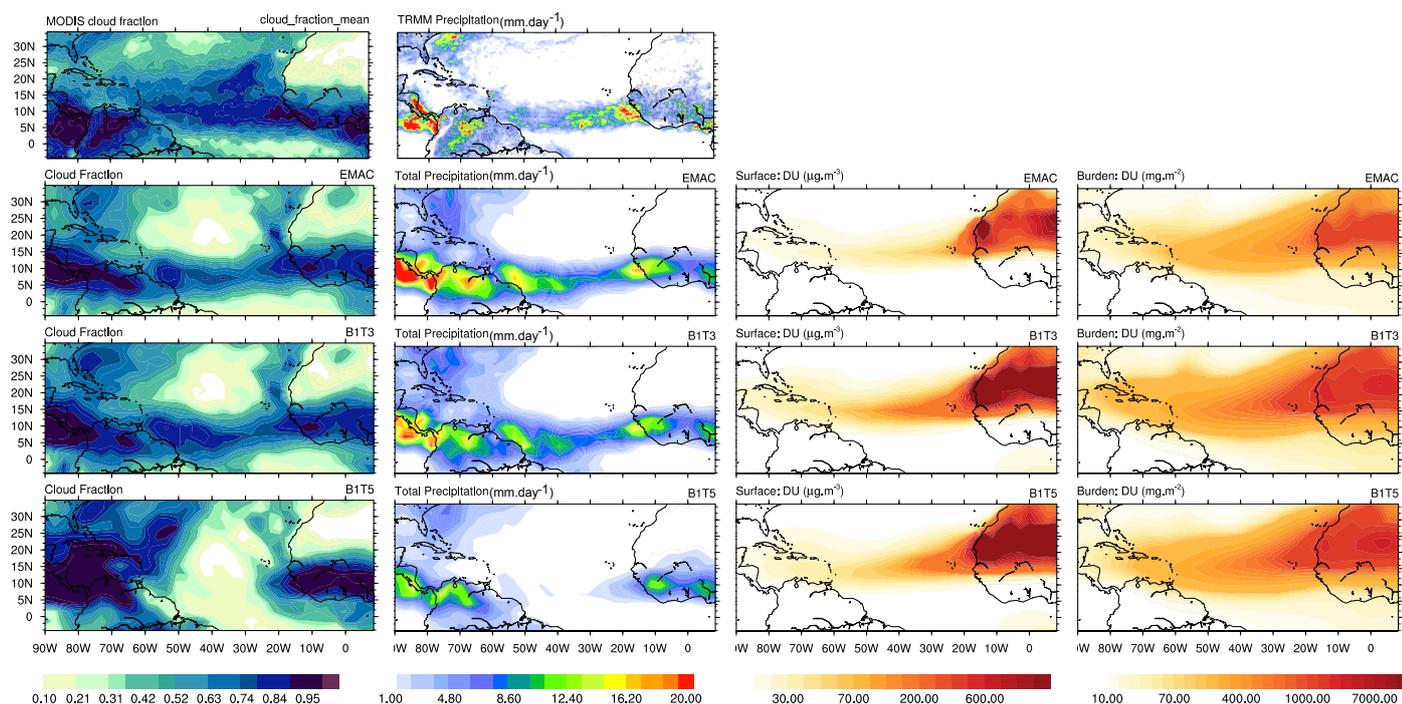
Figure 10. (Top) MODIS cloud fraction and TRMM precipitation (monthly mean); (below) EMAC results (from left to right) cloud fraction, precipitation, surface dust concentration, and dust burden for different convection schemes (2nd–4th row) highlighted in Table 2. The model precipitation and cloud cover agrees for our EMAC set-up best with TRMM and MODIS observations with the ECMWF and TIEDTKE convection schemes.
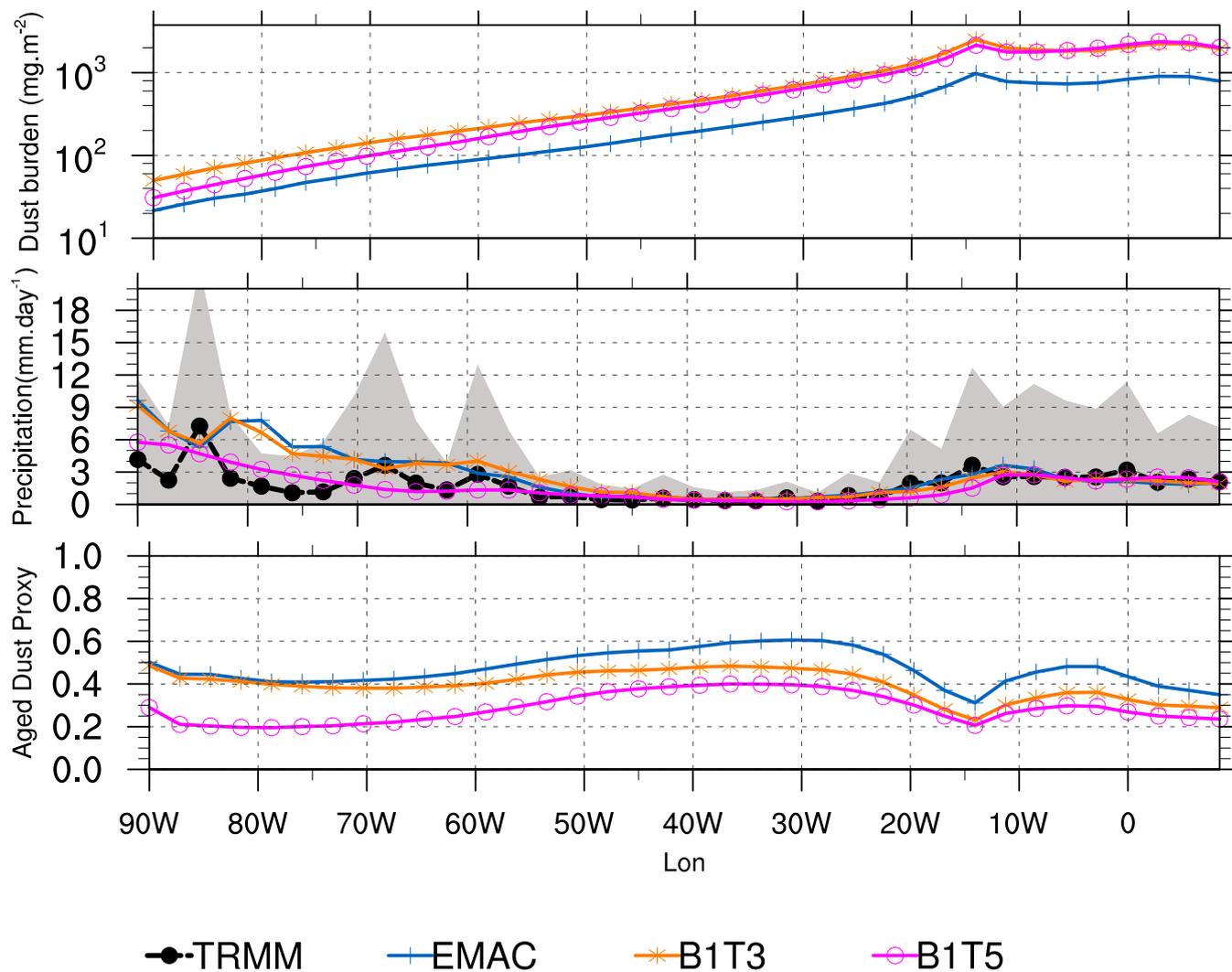
Figure 11. Comparison of observed and calculated meridional means over the dust outflow over the Atlantic Ocean region (10°−25°N) for: (Top) dust burden, (middle) precipitation, (bottom) aged dust proxy (ADP) for July 2009 (monthly mean). The ADP represents the ratio between aged and non-aged dust particles. The shaded area represents one standard deviation of the TRMM-precipitation.
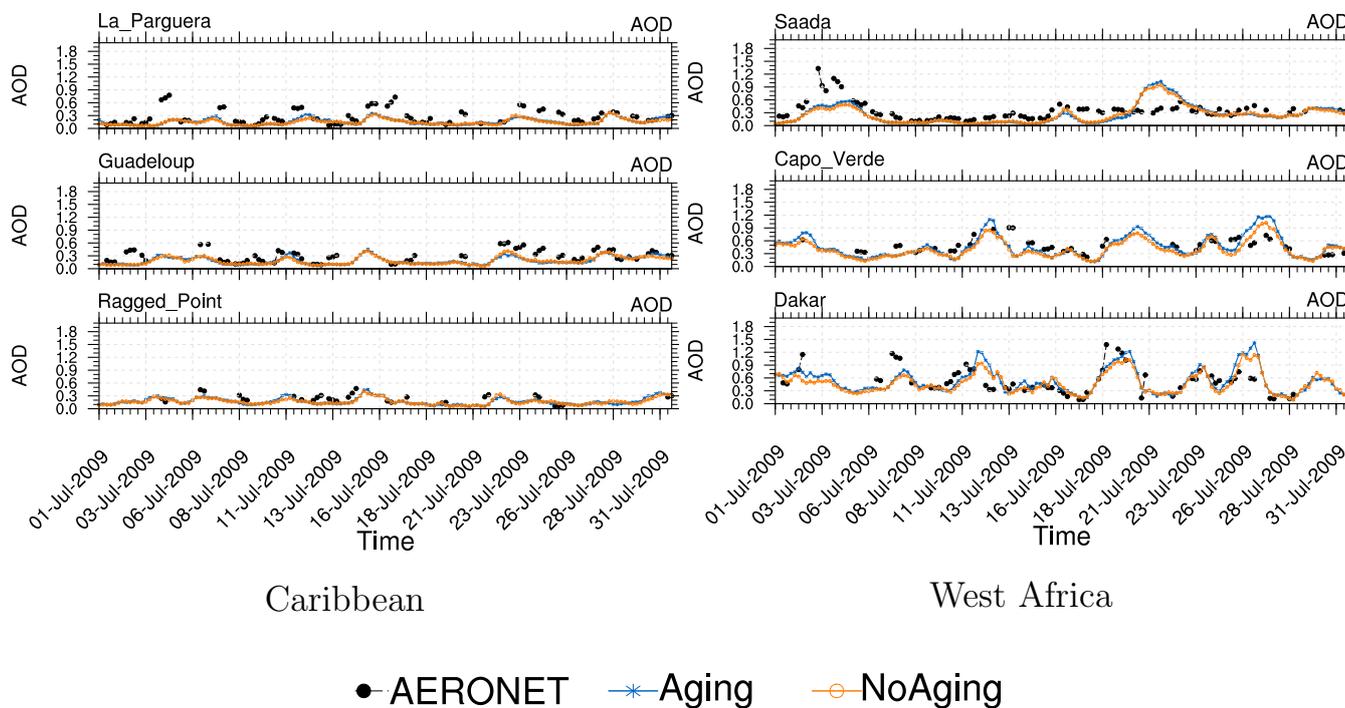
Figure 12. Comparison of observed (AERONET) and calculated AOD for western African and the Caribbean and for two EMAC simulations that include and exclude aging (labeled "Aging" and "No aging", respectively).
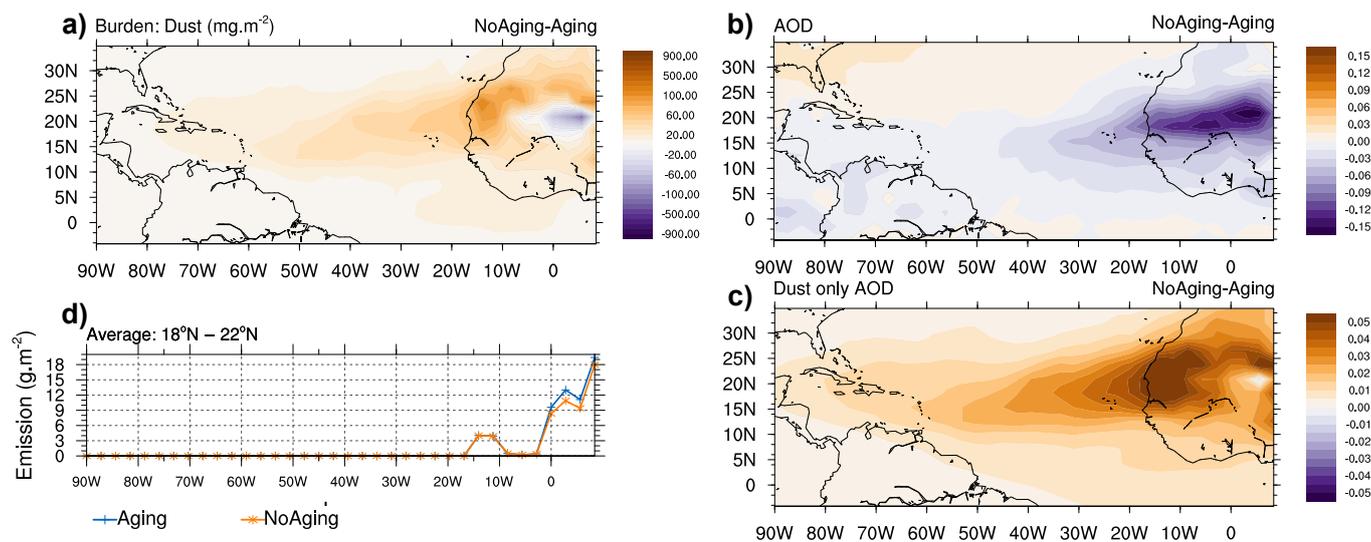

Figure 13. EMAC results (monthly mean) for two simulations that include and exclude aging (labeled "Aging" and "No aging", respectively). (a) difference in dust burden, (b) difference in AOD, (c) dust emission averaged over the region from $18°$-$22°$N for both simulations, (d) difference in "dust only AOD". "Aging" is the reference case. The difference shows the results of the "No Aging" minus "Aging" case.

Atmospheric
Chemistry
and Physics
Discussions
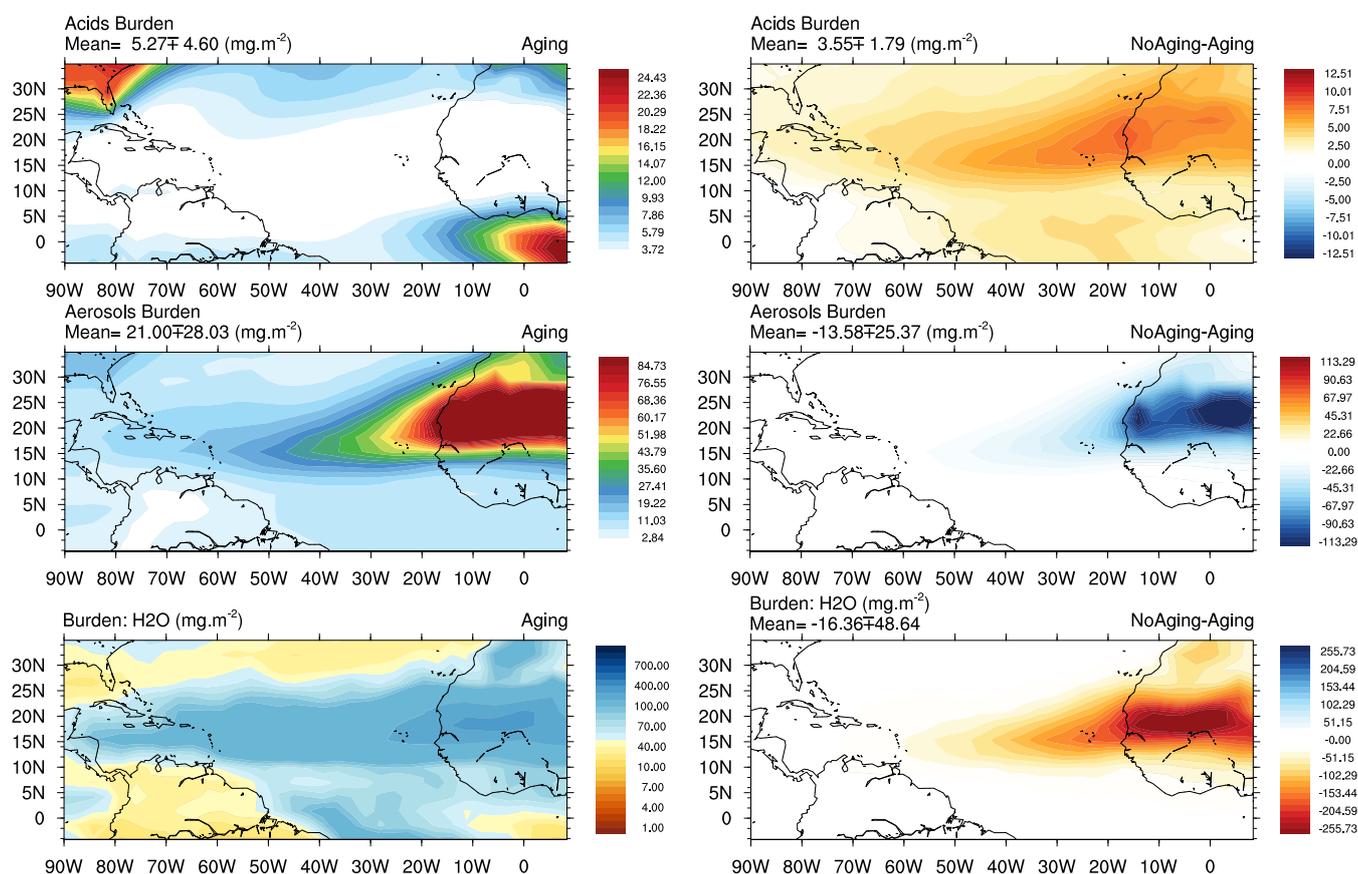
Figure 14. (Top) burden of lumped inorganic gas-phase acids (sum of $HCl+HNO_3+H_2SO_4$), (middle) burden of lumped aerosols (sum of $SO_4^{2-} + HSO_4^- + NO_3^- + NH_4^+ + Cl^- + Na^+ + Ca^{2+} + K^+ + Mg^{2+}$), (bottom) burden of aerosol associated water mass (monthly mean). (Left column) reference simulation (Aging case), (right column) difference between reference and the "No Aging" case. Note the inverted color scales for the bottom two panels, where higher aerosol water mass is shown in blue and lower in red.

Atmospheric
Chemistry
and Physics
Discussions
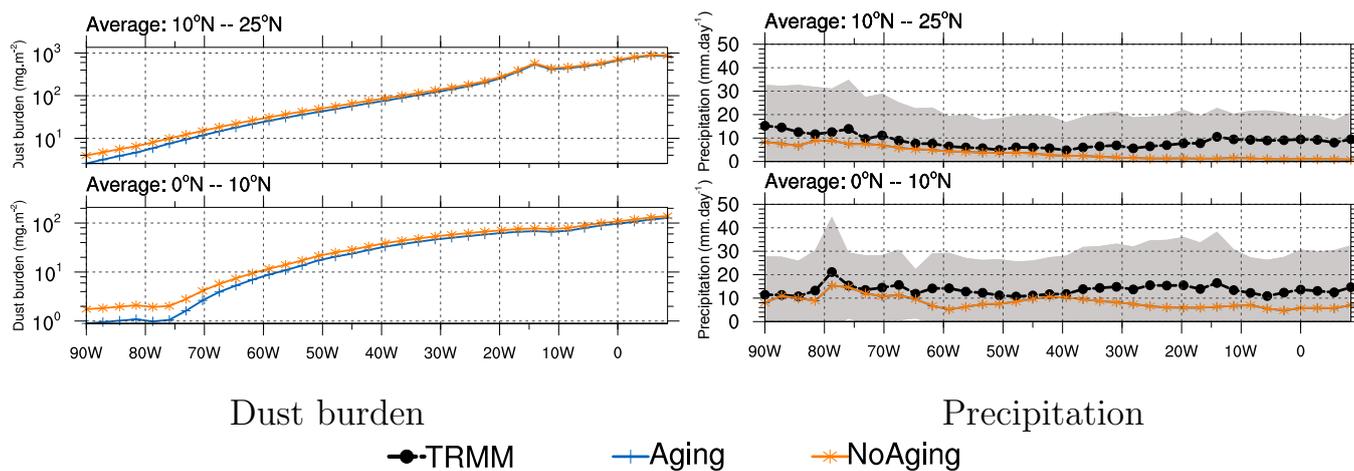
Figure 15. (Left) Dust burden, (right) precipitation for different regions: (Top) dust transport over the Atlantic Ocean zone, (bottom) dust-ITCZ zone $0°$ to $10°$N. The shaded area represents one standard deviation of TRMM precipitation. The results show the long-term average of the entire evaluation period 2000-2012.